Mutagen., 41, 253-259 (2003).
59) N. Toyoda-Hokaiwado, T. Inoue, K. Masumura, H. Hayashi, Y. Kawamura, Y. Kurata, M. Takamune, M. Yamada, H. Sanada, T. Umemura, A. Nishikawa and T. Nohmi, Integration of *in vivo* genotoxicity and short-term carcinogenicity assays using F344 gpt delta transgenic rats: *in vivo* mutagenicity of 2,4-diaminotoluene and 2,6-diaminotoluene structural isomers, *Toxicol. Sci.*, **114**, 71-78 (2010).

PROFILE

深町　勝巳
名古屋市立大学大学院医学研究科
分子毒性学分野
助教
博士（薬学）

静岡県立大学大学院薬学研究科修了、国立がんセンター研究所、米国National Cancer institute/National Institutes of Health を経て名古屋市立大学大学院医学研究科助手/助教。

酒々井　眞澄
名古屋市立大学大学院医学研究科
分子毒性学分野
教授
博士（医学）

1986年岐阜薬科大学製造薬学科卒業、1992年岐阜大学医学部卒業、1996年同大学大学院医学研究科博士課程修了（病理学第1講座）、同年国立がんセンター研究所（発がん研究部）リサーチレジデント、1998年岐阜大学医学部附属病院（第1内科）医員、1999年コロンビア大学医学部がんセンター博士研究員、2002年琉球大学大学院医学研究科（腫瘍病理学）助教授、2006年岐阜薬科大学（分子薬物治療学）教授、2010年名古屋市立大学大学院医学研究科（分子毒性学）教授。内閣府食品安全委員会新開発食品専門調査会専門委員。

徐　結荀
名古屋市立大学
津田特任教授研究室
研究員
博士（医学）

1984年上海医科大学卒業、2003年京都大学大学院医学研究科単位取得満期退学、2010年名古屋市立大学大学院医学研究科博士課程修了、1984～1997年中国安徽医科大学、2003～2005年中国合肥工業大学、助手、講師、助教授として勤め、現在、名古屋市立大学津田特任教授研究室、博士研究員。

津田　洋幸
名古屋市立大学
津田特任教授研究室
特任教授
医学博士

1969年名古屋市立大学医学部卒業、1975年助手、1983年講師、1989年藤田保健衛生大学医学部第二病理学教室助教授、1993年国立ガンセンター研究所化学療法部部長（研究内容は化学発がん）、2003年名古屋市立大学大学院医学研究科分子毒性学分野教授、2009年特任教授。その間カナダ・トロント大学病理学教室、ドイツ国立癌研究センター（ハイデルベルグ）に留学。専門は実験腫瘍学。とくに化学物質による発がん機序、環境発がん物質の*in vivo* 短期スクリーニングモデルの開発、乳蛋白のラクトフェリンの大腸発がん予防作用を動物とヒト介入試験で明らかにした。最近では活性型Kras遺伝子をラットに導入して、世界で初めてのラット膵管がんモデルを確立した。またナノマテリアルの肺発がんリスク研究によって、マクロファージを介する発がん機序を明らかにした。現在炭素ナノマテリアル（フラーレン、カーボンナノチューブ等）の発がんリスクの研究を行っている。
厚生労働省・変異原性試験等結果検討特別会議委員、内閣府食品安全委員会農薬専門調査会確認評価委員、国際癌研究機構（WHO International Agency for Research on Cancer）・発がん物質リスク評価モノグラフ諮問委員（1998、2003、2008）。

The Journal of Toxicological Sciences (J. Toxicol. Sci.)
Vol.35. No.2. 265-270, 2010

Letter

Serum level of expressed in renal carcinoma (ERC)/ mesothelin in rats with mesothelial proliferative lesions induced by multi-wall carbon nanotube (MWCNT)

Yoshimitsu Sakamoto[1], Dai Nakae[1,2], Yoshiaki Hagiwara[3,4], Kanako Satoh[1], Norio Ohashi[1], Katsumi Fukamachi[5], Hiroyuki Tsuda[5], Akihiko Hirose[6], Tetsuji Nishimura[7], Okio Hino[3] and Akio Ogata[1]

[1]Department of Environmental Health and Toxicology, Tokyo Metropolitan Institute of Public Health, 3-24-1 Hyakunin'cho, Shin'juku-ku, Tokyo 169-0073, Japan
[2]Tokyo University of Agriculture, 1-1-1 Sakuragaoaka, Setagaya-ku, Tokyo, 156-8502, Japan
[3]Department of Pathology and Oncology, Juntendo University School of Medicine, 2-1-1 Hongo, Bunkyo-ku, Tokyo 113-8421, Japan
[4]Immuno-Biological Laboratory Co., Ltd., 1091-1 Naka, Fujioka, Gunma 375-0005, Japan
[5]Department of Molecular Toxicology, Nagoya City University, 1 Kawasumi, Mizuho-cho, Mizuho-ku, Nagoya, Aichi 467-8601, Japan
[6]Divisions of Risk Assessment, Biological Safety Research Center and [7]Environmental Chemistry, National Institute of Health Sciences, 1-18-1 Kamiyoga, Setagaya-ku, Tokyo 158-8501, Japan

(Received November 5, 2009; Accepted December 30, 2009)

ABSTRACT — Expressed in renal carcinoma (ERC)/mesothelin is a good biomarker for human mesothelioma and has been investigated for its mechanistic rationale during the mesothelioma development. Studies are thus ongoing in our laboratories to assess expression of ERC/mesothelin in sera and normal/proliferative/neoplastic mesothelial tissues of animals untreated or given potentially mesothelioma-inducible xenobiotics, by an enzyme-linked immunosorbent assay (ELISA) for N- and C-(terminal fragments of) ERC/mesothelin and immunohistochemistry for C-ERC/mesothelin. In the present paper, we intend to communicate our preliminary data, because this is the first report to show how and from what stage the ERC/mesothelin expression changes during the chemical induction of mesothelial proliferative/neoplatic lesions. Serum N-ERC/mesothelin levels were 51.4 ± 5.6 ng/ml in control male Fischer 344 rats, increased to 83.6 ± 11.2 ng/ml in rats given a single intrascrotal administration of 1 mg/kg body weight of multi-wall carbon nanotube (MWCNT) and bearing mesothelial hyperplasia 52 weeks thereafter, and further elevated to 180 ± 77 ng/ml in rats similarly treated and becoming moribund 40 weeks thereafter, or killed as scheduled at the end of week 52, bearing mesothelioma. While C-ERC/mesothelin was expressed in normal and hyperplastic mesothelia, the protein was detected only in epithelioid mesothelioma cells at the most superficial layer. It is thus suggested that ERC/mesothelin can be used as a biomarker of mesothelial proliferative lesions also in animals, and that the increase of levels may start from the early stage and be enhanced by the progression of the mesothelioma development.

Key words: Serum mesothelin, Rat, MWCNT, Mesothelial proliferative lesions

INTRODUCTION

Mesothelioma is a highly aggressive malignant tumor and developed in people previously exposed to asbestos, after a long latency period of 30-40 years. It is desired to establish a biomarker that can identify potential patients with early stage tumors or even as yet without tumors among the high-risk population.

Expressed in renal carcinoma (ERC)/mesothelin is a product of the *Erc* gene discovered in renal carcinomas of the Eker rats (Hino *et al.*, 1995) and confirmed as a homolog of the human *mesothelin/megakaryocyte poten-*

Correspondence: Yoshimitsu Sakamoto (E-mail: Yoshimitsu_Sakamoto@member.metro.tokyo.jp)

coating factor gene (Hino, 2004; Yamashita *et al.*, 2000). A 71-kDa glycosylphosphatidylinositol anchor-type membranous protein is produced and physiologically cleaved by a furin-like protease to yield a membrane-binding 40-kDa C-terminal (C-ERC/mesothelin) and a secreting 31-kDa N-terminal (N-ERC/mesothelin) fragments (Chang and Pastan, 1996; Maeda and Hino, 2006; Yamaguchi, *et al.*, 1994). ERC/mesothelin is a useful marker for human mesothelioma cases (Hino *et al.*, 2007; Maeda and Hino, 2006) and its specific enzyme-linked immunosorbent assay (ELISA) system has been developed (Hagiwara *et al.*, 2008; Nakaishi *et al.*, 2007) for the clinical use (Maeda and Hino, 2006; Shiomi, *et al.*, 2006, 2008; Tajima *et al.*, 2008). The most important question is as to whether ERC/mesothelin can be efficient also in the early phase of the mesothelioma development, and studies are ongoing in our laboratories to assess ERC/mesothelin levels in animals untreated or given potentially mesothelioma-inducible xenobiotics.

We preliminarily assessed ERC/mesothelin levels using the samples of our previous study demonstrating the induction of mesothelial proliferative lesions in male Fisher 344 rats given multi-wall carbon nanotube (MWCNT) (Sakamoto *et al.*, 2009) In the present paper, we intend to communicate this preliminary data, despite its very limited sample numbers, because this is the first report to show how and from what stage the ERC/mesothelin expression changes during the chemical induction of mesothelial proliferative/neoplatic lesions.

MATERIALS AND METHODS

Ethical consideration of the experiments

An experimental protocol was approved by the Experiments Regulation/Animal Experiment Committees of the Tokyo Metropolitan Institute of Public Health for its scientific and ethical appropriateness, including concern for animal welfare, with strict obedience to domestically and internationally applicable declarations, laws, guidelines and rules.

Samples

Male Fisher 344 rats were purchased at their age of 4 weeks old from Charles River Laboratories Japan Inc. (Kanagawa, Japan) and maintained in our animal room (24-25°C, 50-60% relative humidity, 10 times/hr air ventilation and 12-hr light/dark cycle) until use.

Normal rat samples

Serum samples were obtained from 3, 1 and 2 untreated rats at their ages of 11, 42 and 81 weeks old, respectively.

Vehicle/MWCNT-treated rat samples

As detailed elsewhere (Sakamoto *et al.*, 2009), rats were given a single intrascrotal administration of 1 ml/kg body weight of vehicle (2% carboxymethylcellulose) or 1 mg/kg body weight of MWCNT at the age of 12 weeks old and left untreated for up to 52 weeks. In the present study, 9 samples were used: 3 from vehicle-treated rats killed as scheduled at the end of week 52, without any mesothelial changes; 3 from MWCNT-treated rats similarly killed, with mesothelial hyperplasias but without mesotheliomas; and 3 from other MWCNT-treated animals, 1 killed as moribund at week 40 and 2 killed as scheduled at the end of week 52, with early and advanced stages mesotheliomas and hemorrhagic ascites. Serum samples and in the last case an ascites sample were obtained at the time of the autopsy, and 10% neutrally buffered formalin-fixed, paraffin-embedded, mesothelial tissue samples were routinely prepared.

ERC/mesothelinin ELISA assay

Serum and ascites ERC/mesothelin levels were analyzed using rat N- and C-ERC/mesothelin assay kits (Immuno-Biological Laboratories [IBL] Co., Ltd., Gunma, Japan) adapting from the method of Hagiwara *et al.* (2008), the detection limit being 0.1 ng/ml. A 6-µl aliquot was diluted with 234 µl of phosphate-buffered saline containing 1% bovine serum albumin and 0.05% Tween 20. Assays were conducted according to the manufacturer' instruction to measure an optical density at 450 nm. Each sample was assessed in duplicate.

Histology and C-ERC/mesothelin immunohistochemistry

Two serial, 4-µm-thick sections were prepared and deparaffinized. One was processed through a routine hematoxylin and eosin (HE) staining procedure and histgtologically examined. The other was heated in 10 mM citrate buffer, pH 6.0, treated with 3% hydrogen peroxide, incubated with a primary anti-rat C-ERC/mesothelin antibody (IBL) overnight at 4°C, washed with tris-buffered saline, and re-incubated using an Envision system (DAKO Japan Company, Limited, Tokyo, Japan). Signals were visualized by 3,3'-diaminobenzidine, and the sections were counter-stained with hematoxylin.

Statistical analysis

Statistical significance of intergroup difference for the N-ERC/mesothelin level was assessed using Student's *t*-test, and *p*-values less than 0.05 were considered significant.

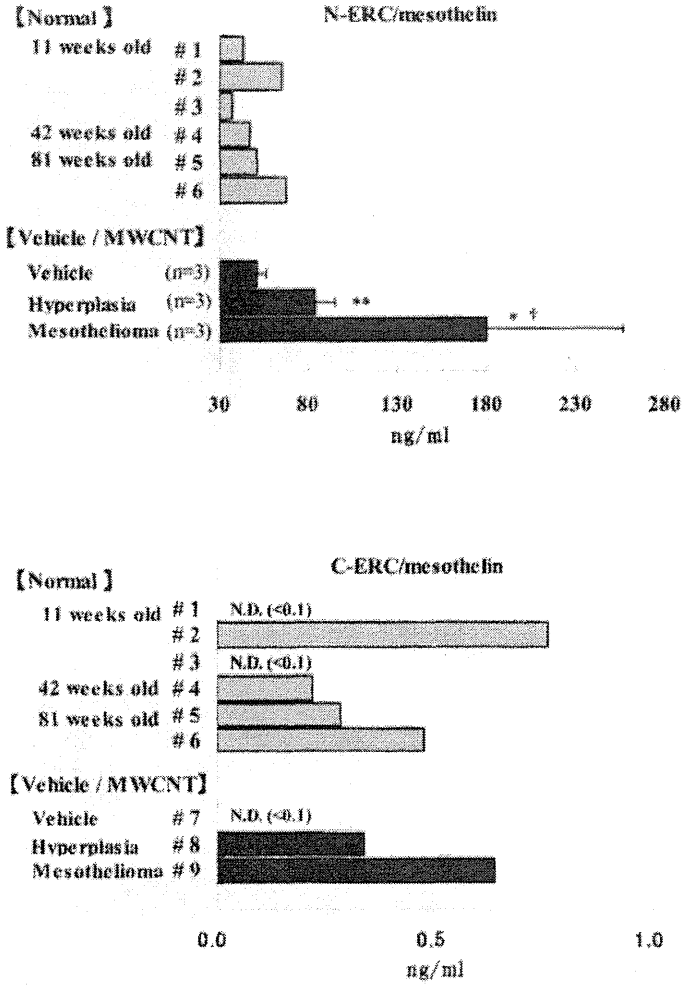

Fig. 1. Serum levels of A, N-ERC/mesothelin and B, C-ERC/mesothelin. Each data is a mean of duplicate assays. #1- #6 in Fig. A and #1- #9 in Fig. B show sample numbers. "N.D.", not detectable, indicates that the data was below the detection limit of 0.10 ng/ml. Values of N-ERC/mesothelin of samples from vehicle, hyperplasia and mesothelioma groups in Fig. B represent the means ± S.D. (n = 3).
Statistical significant difference by Student's t-test: $^{*}P < 0.05$, $^{**}P < 0.01$ as compared from the vehicle group and $^{\dagger}P < 0.05$ as compared from the hyperplastic group.

RESULTS AND DISCUSSION

Serum N-ERC/mesothelin levels of the normal rats were 43.4, 65.1 and 37.3 ng/ml, 47.1 ng/ml and 51.1 and 67.5 ng/ml; while those of C-ERC/mesothelin were < 0.1, 0.8 and < 0.1 ng/ml, 0.2 ng/ml and 0.3 and 0.5 ng/ml; for 11, 42 and 81 weeks or their ages, respectively (Fig. 1). These were respectively within the same range, and the N-ERC/mesothelin levels were substantially higher than the C-ERC/mesothelin levels. No apparent age-dependent changes were obtained for either fragment.

Serum N-(n = 3) and C-(n = 3) ERC/mesothelin levels of the vehicle-treated rat was 51.4 ± 5.6 ng/ml and < 0.1 ng/ml, respectively, within the normal ranges, whereas serum N-ERC/mesothelin levels of MWCNT-treated rats were increased by the induction of mesothelial hyperpla-

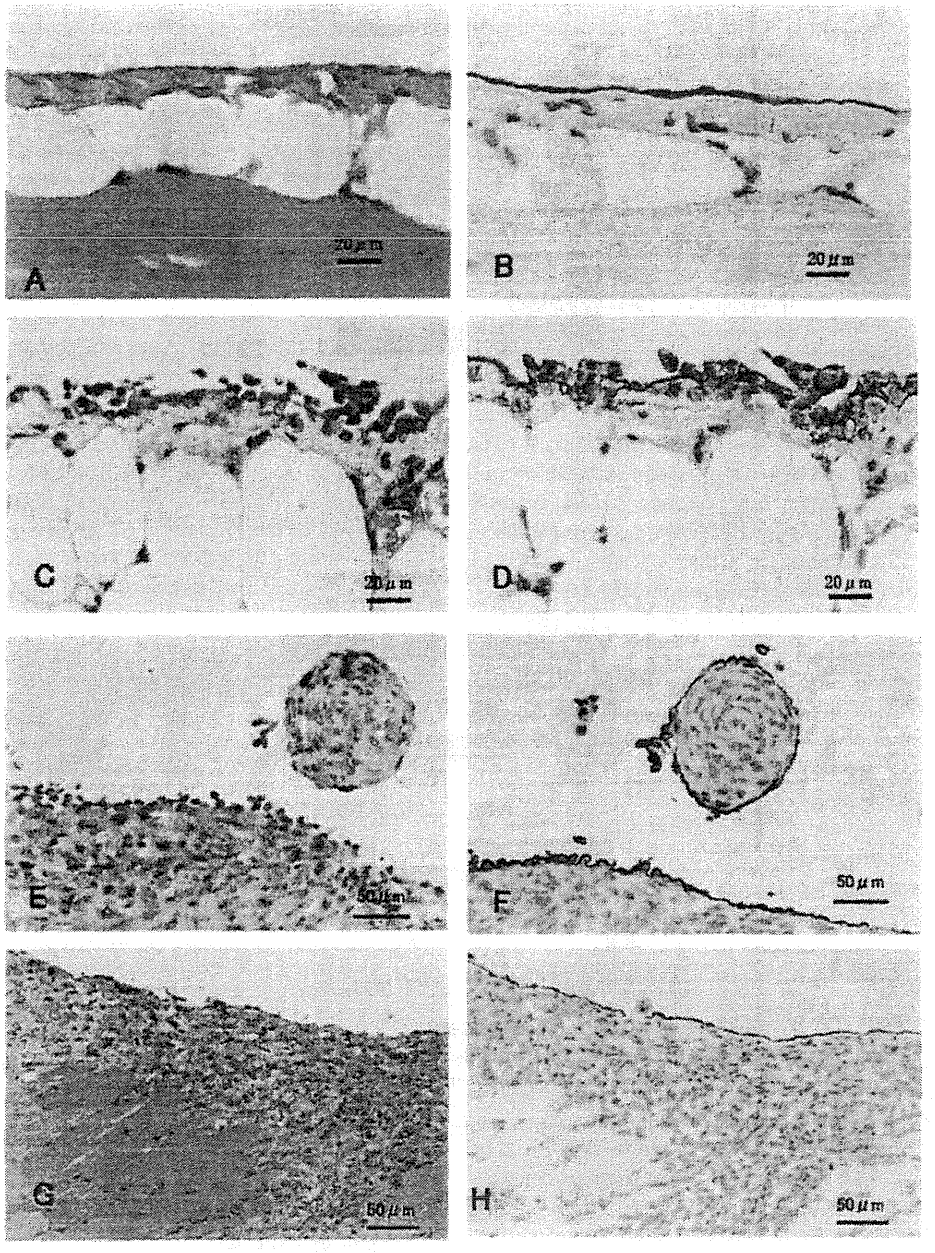

Fig. 2. Representative histology and C-ERC/mesothelin immunohistochemistry.
A, intact mesothelia in the parietal peritoneum of the vehicle-treated rat, HE; B, A's serial section, C-ERC/mesothelin; C, a mesothelial hyperplasia in the retroperotineal fat tissue of the MWCNT-treated rat, HE; D, C's serial section, C-ERC/mesothelin; E, an early-stage epithelioid/polypoid type mesothelioma in retroperotineal fat tissue of the other MWCNT-treated rat, HE; F, E's serial section, C-ERC/mesothelin; G, an advanced-stage mostly-sarcomatoid/invasive-nodular type mesothelioma in the diaphragm of the MWCNT-treated rat (the same animal as E/F), HE; H, G's serial section, C-ERC/mesothelin. Bars with their lengths are inserted to indicate magnifications.

sia (83.6 ± 11.2 ng/ml) and further by that of mesothelioma (179 ± 77 ng/ml; 3,004 ± 665 ng/ml in ascites) (Fig. 1). Serum N-ERC/mesothelin levels in experimental animals have only been assessed in Eker and Wistar rats and nude mice, untreated or transplanted with a rat mesothelioma cell line, MetEt-40 (Hagiwara *et al.*, 2008; Nakaishi *et al.*, 2007). The present data for the first time demonstrates that serum N-ERC/mesothelin level was increased already at the stage of preneoplastic, mesothelial hyperplasia and further increased by the chemical induction of mesothelioma. This may be in line with the recent findings that elevated serum mesothelin is detected before the development of grossly visible carcinoma lesions in a rat pancreatic carcinoma models (Fukamachi *et al.*, 2009). In human mesothelioma, it has been reported that N-ERC/mesothelin level increased with the stage went up of epithelioide type mesothelioma in human case (Shiomi *et al.*, 2008). It is not known, however, how N-ERC/mesothelin levels change in the stage of preneoplasia at this moment. Large-scaled, detailed investigations using the MWCNT-mesothelioma model are ongoing in our laboratories.

Serum C-ERC/mesothelin levels of MWCNT-treated rats were 0.4 and 0.6 ng/ml, within the normal/vehicle range (Fig. 1B). This is in accordance with the previous finding in nude mice transplanted with MetET-40 (Hagiwara *et al.*, 2008), and can be attributed to the membrane-binding property of C-ERC/mesothelin (Maeda and Hino, 2006). Ascites level of C-ERC/mesothelin in the mesothelioma case was slightly increased to 10.9 ng/ml (Fig. 1B). This is speculated to result from a release of C-ERC/mesothelin by phosphatidylinositol-specific phospholipase C (Chang and Pastan, 1996) or a contamination of desquamated mesothelioma cells.

Immuohistochemical C-ERC/mesothelin signals were constantly detected in cell membranes. C-ERC/mesothelin was detected in intact (Figs. 2A and B) and hyperpastic (Figs. 2C and D) mesothelia. Taken the ELISA data together, it might be possible that the ERC/mesothelin level starts increased from the preneoplastic stage.

C-ERC/mesothelin was found only in epithelioid (mesothelioid) tumor cells present at the most superficial layer of early-stage, epithelioid/polypoid (Figs. 2E and F) and advanced-stage, mostly-sarcomatoid/invasive-nodular (Figs. 2G and H) types of mesotheliomas. In humans, epithelioid types, but not sarcomatoid types or sarcomatoid components of biphasic (mixed) types, immunohistochemically express C-ERC/mesothelin (Chang and Pastan, 1996; Shiomi *et al.*, 2008; Ordóñez, 2003). Accordingly, serum N-ERC/mesothelin levels were only slightly increased or often unchanged in sarcomatoid and biphasic types, in contrast to the epithelioid type (Hassan *et al.*, 2006; Shiomi *et al.*, 2008). The present findings suggest that the increaseof ERC/mesothelin levels in mesotheliomas may be a universal event for all types and stages, and that C-terminal fragments may become unproduced or changed its tertiary structure and/or epitope construction by the neoplastic conversion.

In conclusion, the present data suggests that ERC/mesothelin can be used as a biomarker of mesothelial proliferative lesions also in animals, and that its increase of its levels may start from the early stage and be enhanced by the progression of the mesothelioma development.

ACKNOWLEDGMENTS

This work was supported in part by a research budget of the Tokyo Metropolitan Government, Japan, and Grants-in-Aid for Scientific Research from the Ministry of Health, Labour and Welfare of Japan, from the Japan Society for the Promotion of Science, and from the Ministry of Education, Culture, Sports, Science and Technology of Japan. This study was also partially supported by a consignment expense for Molecular Imaging Program on "Research Base for PET Diagnosis" from the Ministry of Education, Culture, Sports, Science and Technology of Japan.

REFERENCES

Chang, K. and Pastan, I. (1996): Molecular cloning of mesothelin, a differentiation antigen present on mesothelium, mesotheliomas, and ovarian cancers. PNAS USA, **93**, 136-140.

Fukamachi, K., Tanaka, H., Hagiwara, Y., Ohara, H., Joh, T., Iigo, M., Alexander, D.B., Xu, J., Long, N., Takigahira, M., Yanagihara, K., Hino, O., Saito, I. and Tsuda, H. (2009): An animal model of preclinical diagnosis of pancreatic ductal carcinomas. Biochem. Biophys. Res. Commun., **390**, 636-641.

Hagiwara, Y., Hamada, Y., Kuwahara, M., Maeda, M., Segawa, T., Ishikawa, K. and Hino, O. (2008): Establishment of a novel specific ELISA system for rat N- and C-ERC/mesothelin. Rat ERC/mesothelin in the body fluids of mice bearing mesothelioma. Cancer Sci., **99**, 666-670.

Hassan, R., Remaley, A.T., Sampson, M.L., Zhang, J., Cox, D.D., Pingpank, J., Alexander, R., Willingham, M., Pastan, I. and Onda, M. (2006): Detection and quantitation of serum mesothelin, a tumor marker for patients with mesothelioma and ovarian cancer. Clin. Cancer Res., **12**, 447-453.

Hino, O., Kobayashi, E., Nishizawa, M., Kubo, Y., Kobayashi, T., Hirayama, Y., Takai, S., Kikuchi, Y., Tsuchiya, H., Orimoto, K., Kajino, K., Takahata, T. and Hitani, H. (1995): Renal carcinogenesis in the Eker rat. J. Cancer Res. Clin. Oncol., **121**, 602-605.

Hino, O. (2004): Multistep renal carcinogenesis in the Eker (*Tsc2* gene mutant) rat model. Curr. Mol. Med., **4**, 807-811.

Hino, O., Shiomi, K. and Maeda, M. (2007): Diagnostic biomarker of asbestos-related mesothelioma: example of translational research. Cancer Sci., **98**, 1147-1151.

Maeda, M. and Hino, O. (2006): Molecular tumor markers for asbestos-related mesothelioma: serum diagnostic markers. Pathol. Int., **56**, 649-654.

Ordóñez, N.G. (2003): Value of mesothelin immunostaining in the diagnosis of mesothelioma. Mod. Pathol., **16**, 192-197.

Nakaishi, M., Kajino, K., Ikesue, M., Hagiwara, Y., Kuwahara, M., Mitani, H., Horikoshi-Sakuraba, Y., Segawa, T., Kon, S., Maeda, M., Wang, T., Abe, M., Yokoyama, M. and Hino, O. (2007): Establishment of the enzyme-linked immunosorbent assay system to detect the amino terminal secretary form of rat Erc/Mesothelin. Cancer Sci., **98**, 659-664.

Sakamoto, Y., Nakae, D., Fukumori, N., Tayama, K., Maekawa, A., Imai, K., Hirose, A., Nishimura, T., Ohashi, N. and Ogata, A. (2009): Induction of mesothelioma by a single intrascrotal administration of multi-wall carbon nanotube in intact male Fischer 344 rats. J. Toxicol. Sci., **34**, 65-76.

Shiomi, K., Miyamoto, H., Segawa, T., Hagiwara, Y., Ota, A., Maeda, M., Takahashi, K., Masuda, K., Sakao, Y. and Hino, O. (2006): Novel ELISA system for detection of N-ERC/mesothelin in the sera of mesothelioma patients. Cancer Sci., **97**, 928-932.

Shiomi, K., Hagiwara, Y., Sonoue, K., Segawa, T., Miyashita, K., Maeda, M., Izumi, H., Masuda, K., Hirabayashi, M., Moroboshi, T., Yoshiyama, T., Ishida, A., Natori, Y., Inoue, A., Kobayashi, M., Sakao, Y., Miyamoto, H., Takahashi, K. and Hino, O. (2008): Sensitive and specific new enzyme-linked immunosorbent assay for N-ERC/mesothelin increases its potential as a useful serum tumor marker for mesothelioma. Clin. Cancer Res., **14**, 1431-1437.

Tajima, K., Hirama, M., Shiomi, K., Ishiwata, T., Yoshioka, M., Iwase, A., Iwakami, S., Yamazaki, M., Toba, M., Tobino, K., Sugano, K., Ichikawa, M., Hagiwara, Y., Takahashi, K. and Hino, O. (2008): ERC/mesothelin as a marker for chemotherapeutic response in patients with mesothelioma. Anticancer Res., **28**, 3933-3936.

Yamaguchi, N., Hattori, K., Oheda, M., Kojima, T., Imai, N. and Ochi, N. (1994): A novel cytokine exhibiting megakaryocyte potentiating activity from a human pancreatic tumor-cell line HPC-Y5. J. Biol. Chem., **269**, 805-808.

Yamashita, Y., Yokoyama, M., Kobayashi, E., Takai, S. and Hino, O. (2000): Mapping and determination of the cDNA sequence of the *Erc* gene preferentially expressed in renal cell carcinoma in the *Tsc2* gene mutant (Eker) rat model. Biochem. Biophys. Res. Commun., **275**, 134-140.

A Medium-Term, Rapid Rat Bioassay Model for the Detection of Carcinogenic Potential of Chemicals

Hiroyuki Tsuda, Mitsuru Futakuchi, Katsumi Fukamachi, Tomoyuki Shirai, Katsumi Imaida, Shoji Fukushima, Masae Tatematsu, Fumio Furukawa, Seiko Tamano and Nobuyuki Ito

Toxicol Pathol 2010; 38; 182 originally published online Jan 15, 2010;
DOI: 10.1177/0192623309356451

Toxicologic Pathology, 38: 182-187, 2010

ISSN: 0192-6233 print / 1533-1601 online
DOI: 10.1177/0192623309356451

A Medium-Term, Rapid Rat Bioassay Model for the Detection of Carcinogenic Potential of Chemicals

HIROYUKI TSUDA,[1,2] MITSURU FUTAKUCHI,[2] KATSUMI FUKAMACHI,[2] TOMOYUKI SHIRAI,[3] KATSUMI IMAIDA,[4] SHOJI FUKUSHIMA,[5] MASAE TATEMATSU,[5] FUMIO FURUKAWA,[6] SEIKO TAMANO,[6] AND NOBUYUKI ITO[3]

[1]*Nanotoxicology Project, Nagoya City University Graduate School of Medical Sciences, 1 Kawasumi, Mizuho-ku, Mizuho-cho, Nagoya 467-8601, Japan*

[2]*Department of Molecular Toxicology, Nagoya City University Graduate School of Medical Sciences, 1 Kawasumi, Mizuho-ku, Mizuho-cho, Nagoya 467-8601, Japan*

[3]*Department of Experimental Pathology and Tumor Biology, Nagoya City University Graduate School of Medical Sciences, 1 Kawasumi, Mizuho-ku, Mizuho-cho, Nagoya 467-8601, Japan*

[4]*Department of Pathology and Host-Defense, Faculty of Medicine, Kagawa University, 1750-1, Ikenobe, Miki-cho, Kita-gun, Kagawa 761-0793, Japan*

[5]*Japan Bioassay Research Center, 2445 Hirasawa, Hadano, Kanagawa 257-0015, Japan*

[6]*Daiyu-kai Institute of Medical Science (DIMS), 64 Goura, Nishiazai, Azai-cho, Ichinomiya 491-0113, Japan*

ABSTRACT

The Ito Liver Model and the Ito Multi-organ Model are used in conjunction and constitute an efficient and rapid bioassay for the identification of both genotoxic and nongenotoxic carcinogenic chemicals. The Ito Liver Model is an 8-week bioassay system that uses the number and size of foci of hepatocytes positive for glutathione S-transferase placental form (GST-P) as the end-point marker. One hundred fifty-nine compounds were tested using the Ito Liver Model: 61 of 66 hepatocarcinogens tested positive, and 10 of 43 nonliver carcinogens were also positive. The false-positive detection of noncarcinogens was low; a single false-positive result was obtained from the 50 noncarcinogens tested. Since more than half of all known carcinogens are hepatocarcinogens in rodents, the initial 8-week bioassay is able to detect most carcinogens. The Ito Multi-organ Model is a 28-week bioassay system for the detection of carcinogens that were not identified by the Ito Liver Model. Results are evaluated by preneoplastic and neoplastic lesions in major organs. Forty-four compounds were tested using the Ito Multi-organ Model: 17 out of 17 liver carcinogens were positive, and 19 out of 22 (86%) nonliver carcinogens were positive. None of the five noncarcinogens tested positive.

Keywords: medium-term bioassay; carcinogens; liver GST-P; multi-organ.

INTRODUCTION

Identification and control of carcinogens in the environment are of prime importance to reduce cancer risk in humans. Long-term chronic administration assays for the detection of carcinogenicity and toxicity using rodents have been the standard for the evaluation of the carcinogenic potential of chemicals. The requirements call for testing in two rodent species, usually rats and mice, of each sex, at three dose levels (zero, low, middle, and high) of the test compound for 2 years.

Although this standard has long been used worldwide, 2-year carcinogenicity studies are too costly to test all the chemicals being introduced into the environment. Furthermore, there is political pressure to decrease the number of animals used for carcinogenicity testing because of animal welfare considerations (Ashby and Tennant 1991). A guideline proposed by the International Conference on Harmonization (ICH) recommends reducing long-term protocols by utilizing only one rodent species and replacing the second long-term rodent assay with an alternative bioassay (ICH Steering Committee 1997).

It is known that mutagenicity does not always correlate with carcinogenicity, and there are a variety of chemicals in use, typically represented by pesticides and herbicides, that are not mutagenic but are carcinogenic. A whole-body animal study is the only method to test the carcinogenic potential of a nongenotoxic chemical. Therefore, any alternative bioassay must be an in vivo, whole-body assay. Our laboratories have focused

Address correspondence to: Hiroyuki Tsuda, Nanotoxicology Project, Nagoya City University Graduate School of Medical Sciences, 1 Kawasumi, Mizuho-ku, Mizuho-cho, Nagoya 467-8601, Japan; e-mail: htsuda@med.nagoya-cu.ac.jp.

These research projects were supported in part by Grants-in-Aid for Cancer Research from the Ministry of Education, Culture, Sports, Science and Technology and the Ministry of Health, Labour and Welfare; a Grant-in-Aid from the Ministry of Health, Labour and Welfare for the 2nd Term Comprehensive 10-Year Strategy for Cancer Control; and grants from the Society for Promotion of Pathology of Nagoya and the Experimental Pathological Research Association, Nagoya, Japan. Portions of this review have been previously published as noted in the text; we have updated the information for 2009.

on the development of a rapid in vivo bioassay system able to detect both genotoxic and nongenotoxic carcinogens.

Since more than half of all known carcinogens are hepatocarcinogens in rodents, we initially focused on establishment of a medium-term liver bioassay system. We developed an 8-week rat liver bioassay, known as the Ito Liver Model, which is able to detect rat hepatocarcinogens with a high degree of accuracy (Shirai, Hirose, and Ito 1999). This protocol is cited in the sixth edition of *Casarett and Doull's TOXICOLOGY* as a potential alternative bioassay (Pitot and Dragan 2001). In addition, we developed a 28-week model, known as the as Ito Multi-organ Model, to detect carcinogens that are not identified by the Ito liver model.

Using the Ito Liver Model in conjunction with the Ito Multi-organ Model, most carcinogens can be identified after 8 weeks, and the remaining carcinogens can be identified after an additional 28 weeks. In the present review, the Ito Liver Model and the Ito Multi-organ Model are briefly described.

Background

In 1976, Solt and Farber developed a protocol in which foci of liver cells expressing an altered repertoire of enzymes could be induced in rats within 4 weeks. Their protocol was based on their observation that in rats treated with diethylnitrosamine (DEN) followed by the hepatocarcinogen 2-acetylaminofluorene (2-AAF), DEN-altered hepatocytes were able to respond to growth stimuli evoked by a two-thirds partial hepatectomy and form distinct foci. In contrast, normal hepatocytes were not able to respond to the growth stimuli because of the toxic effect of 2-AAF. This observation was described as a "selection process" by altered hepatocytes (Solt and Farber 1976). The application of this observation for carcinogen detection was examined by treating rats with test compounds to generate altered hepatocytes followed by feeding with 2-AAF and stimuli to induce hepatocyte proliferation, and the principle of the method was validated: treatment with representative carcinogens resulted in the formation of foci of altered hepatocytes (Tsuda, Lee, and Farber 1980).

In other studies, Peraino and associates reported a two-stage model in which hepatic tumor growth was enhanced by chemicals such as phenobarbital given after initiation with 2-AAF (Peraino et al. 1975, 1977, 1980). Their data suggested that a two-stage approach could be utilized for detection of carcinogenic responses to chemicals: either test compounds could given at the initiation stage followed by appropriate promoting agents or test compounds could be given during the promotion stage after initiation with DEN.

Based on the concepts presented above, we established an assay system to evaluate the hepatocarcinogenicity of chemicals for their promotion potential (Ito et al. 1996, 1997; Ito, Tamano, and Shirai 2003): we used the promotion potential of hepatocarcinogens because almost all carcinogens have a promotion effect when repeatedly administered (Peraino et al. 1975, 1977, 1980). The preneoplastic nature of altered hepatic foci and the usefulness of such lesions as indicators

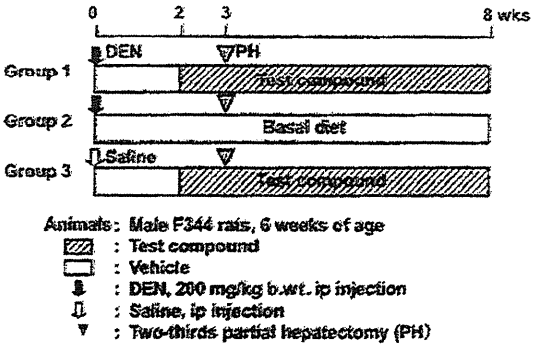

FIGURE 1.—Protocol of Ito Liver Model. Six-week-old male F344 rats are initially given a single intraperitoneal injection of diethylnitrosamine (200 mg/kg) to initiate liver carcinogenesis. Two weeks after initiation, the test compound is administered for 6 weeks. Animals are sacrificed at the end of week 8. All rats are subjected to two-thirds partial hepatectomy on week 3. The end-point marker is glutathione S-transferase placental form-positive (GST-P$^+$) liver cell foci. The numbers and sizes of GST-P$^+$ liver cell foci are analyzed using an image-analyzer and expressed as values per unit liver section (1 cm^2). When values, number, and/or area per unit area of GST-P$^+$ foci are significantly enhanced ($P < .05$) over the control value, a chemical is judged to possess carcinogenic potential for the liver.

of preneoplastic development are now well accepted (Bannasch 1986; Oesterle and Deml 1990; Tatematsu et al. 1977). The phenotypic characteristics of preneoplastic lesions in the liver have been extensively studied, and immunohistochemical staining for glutathione S-transferase placental form (GST-P) was found to be the best marker for visualization of lesions and their quantitative analysis (Ogiso et al. 1985; Tsuda et al. 2003, 1985).

Assay Protocol and Results

Ito Liver Model

Figure 1 shows the protocol employed in Ito's laboratory as a medium-term liver bioassay model. Male F344 male rats, 5 weeks old, are divided into three groups consisting of 15 to 20 animals each. Group 1 is given a single intraperitoneal injection of DEN, 200 mg/kg b.wt., dissolved in saline to initiate hepatocarcinogenesis. After 2 weeks, the rats receive a test compound mixed in the basal diet or drinking water or by repeated intraperitoneal, subcutaneous or intravenous injections. The rats are subjected to two-thirds partial hepatectomy (PH) at the end of week 3. Group 2 is given DEN and PH in the same manner as for group 1, but without administration of the test compound. Group 3 is injected with saline instead of DEN and then subjected to administration of the test compound and PH as in groups 1 and 2 (Figure 1). All animals are sacrificed at the end of week 8. The liver tissues, three to four slices from the cranial and caudal lobes of the right lateral lobe and caudal and/or cranial part of the caudal lobe, are excised and fixed in ice-cold acetone or 4% paraformaldehyde solution in phosphate

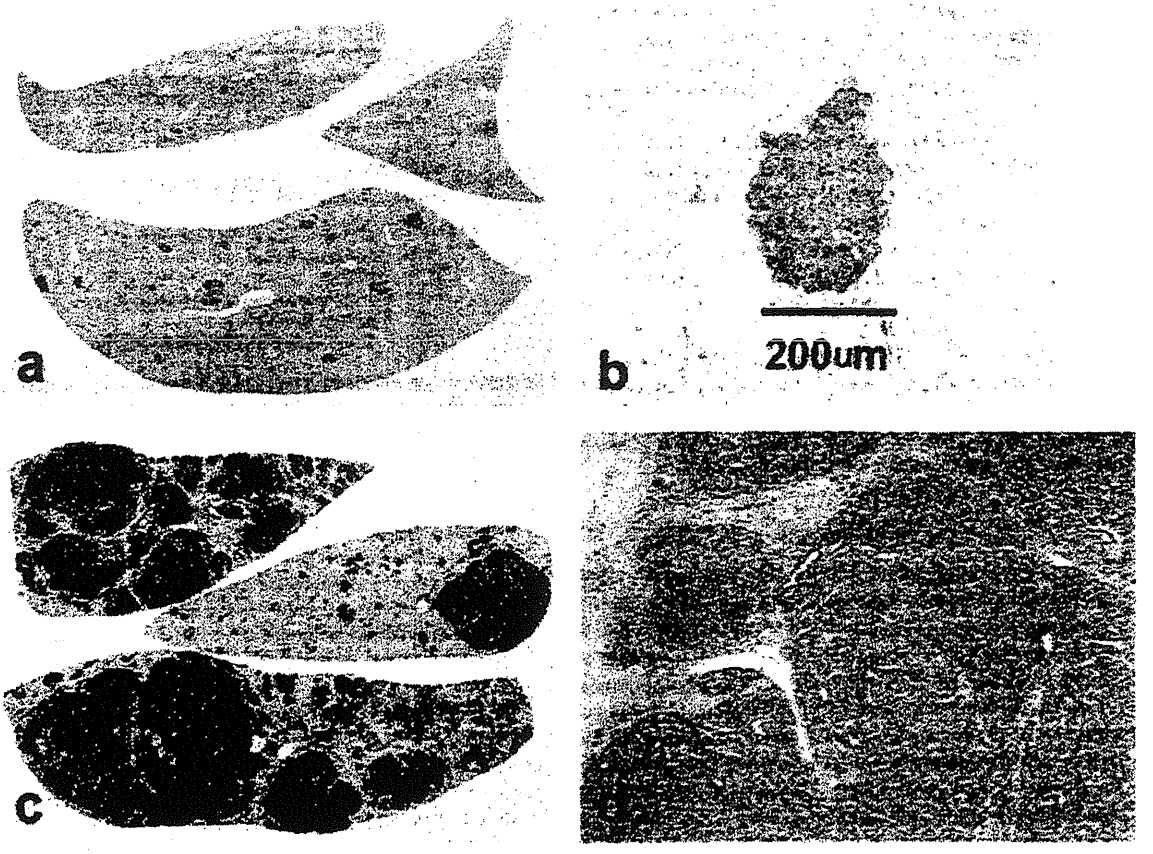

FIGURE 2.—GST-P-positive liver cell foci. Three to four slices from paraffin embedded liver (left) are immunostained with GST-P antibody. Lesions greater than 200μm (right) in diameter are included for counting. GST-P is consistently expressed from small foci to adenomas and hepatocellular carcinomas. A clear correlation between GST-P-positive foci and the incidence of hepatocellular carcinomas can be seen. (a) A low magnification view of a slide from a rat treated with phenobarbital (0.05%, in the diet). (b) Smallest focus included for counting purposes. (c) A low-magnification view of a slide from a rat treated with 2-AAF (0.02%, in the diet). (d) Higher-magnification view of hepatocellular carcinoma: the carcinoma is clearly positive for GST-P.

buffer at pH. 7.4 for subsequent paraffin embedding and immunohistochemical demonstration of GST-P-positive foci (Figure 2). Numbers and areas of GST-P-positive foci more than 0.2 mm^2 in mean diameter are included for measuring by an image processor. The results are assessed by comparing the values between group 1 (DEN-test compounds) and group 2 (DEN alone). Group 3 serves to assay the potential of the test chemicals to induce GST-P-positive foci without prior DEN exposure. Statistical analysis of differences between means is carried out using Student's or Welch's *t*-tests after application of a preliminary *F*-test for equal variance, and scoring of carcinogenicity, promotion, or inhibition is made on the basis of differences in *P*-values between groups; positive = increase at $P < .05$ in either number or area of foci.

Until the protocol was finalized, the following were extensively investigated to maximize the predictive potential of the model (Hasegawa and Ito 1992; Ito et al. 1997, 1992; Shirai 1997; Shirai, Hirose, and Ito 1999):

1. use of PH as a tool for induction of hepatocyte proliferation,
2. the most suitable end-point marker enzyme,
3. whether results with GST-P-positive foci can predict carcinoma development in a dose dependent manner, and
4. specificity of the protocol for detection of carcinogens.

Since PH was introduced by Higgins and Anderson in 1931, it has been extensively employed for investigation of cell proliferation and regeneration. After two-thirds PH, the rodent liver recovers quickly and returns to near preoperative weight

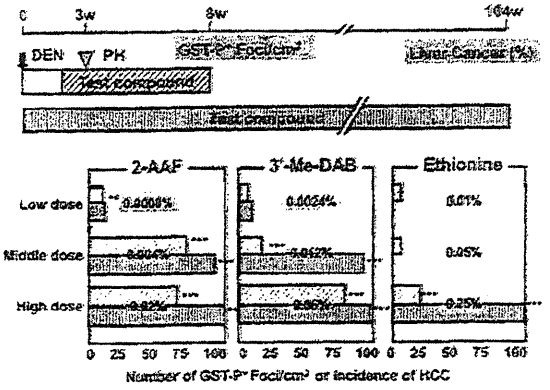

FIGURE 3.—Comparison of GST-P-positive foci and carcinoma. Results obtained from the Ito Liver Model and long-term 2-year studies are shown. Different doses of three representative hepatocarcinogens—2-acetylaminofluorene, 3'-methy-4-diaminoazobenzene, and ethionine—were administered.

within 1 week with peak DNA synthesis at about 24 hr; induction of hepatocyte growth factor appears to be one mechanism by which the liver recovers from PH (Matsumoto and Nakamura 1992). Use of hepatotoxins such as carbon tetrachloride (CCl_4) or D-galactosamine is an alternative method to induce liver cell proliferation. However, neither of these agents stimulates cell proliferation equivalent to PH in our system because induction of cells to enter S-phase of the cell cycle by these chemicals is sluggish (data not shown).

We have not yet elucidated the role of cell proliferation induced by PH at week 3 in the appearance of liver cell foci. It is possible that a majority of carcinogens are toxic to hepatocytes, causing retardation of the compensatory regenerative response to PH by noninitiated hepatocytes, allowing focal expansion of initiated hepatocytes. In this regard, it is known that initiated cells reduce phase I CYP enzyme expression and increase phase II enzyme expression (Liu et al. 2005; Tsuda et al. 1996), and this altered enzyme expression enables them to escape the effects of toxic compounds.

The expression of several different enzymes is altered in liver preneoplastic lesions (Ogawa et al. 1982; Tsuda et al. 1992). We compared the use of a variety of enzyme markers to visualize liver lesions (Tsuda et al. 2003, 1984). GST-P was found to be the most appropriate for practical use and is expressed continuously from the early lesion to the appearance of hepatocellular carcinoma (Kitahara et al. 1984; Tsuda et al. 1996, 2003).

Several studies have shown the validity of using GST-P-positive foci as a surrogate end-point in predicting carcinogenic potential (Ogawa et al. 1982; Tatematsu et al. 1985; Tsuda et al. 1984, 1988). One of these studies is shown in Figure 3. There was a clear correlation between GST-P-positive foci and incidence of hepatocellular carcinomas after administration of different doses of the well-known hepatocarcinogens

TABLE 1.—Results for 159 Compounds in the Ito's Test

	No. of Positive Compounds/Examined (%)			
	Mutagenicity (Ames test)			
Test Compounds	Positive	Negative	Unknown	Total
Liver carcinogen	31/32(97)[a]	29/33(88)[b]	1/1(100)	61/66(92)
Non-liver carcinogen	7/26(27)	2/15(13)	1/2(50)	10/43(23)[c]
Not carcinogenic	0/6(0)	1/42(2)	0/2(0)	1/50(2)

[a] 4,4-Diaminodiphenylmethane gave negative results
[b] Four chemicals, Clofibrate, Di(2-ethylhexyl)adipate, Di(2-ethylhexyl)phthalate, Trichloroacetic acid, gave negative result.

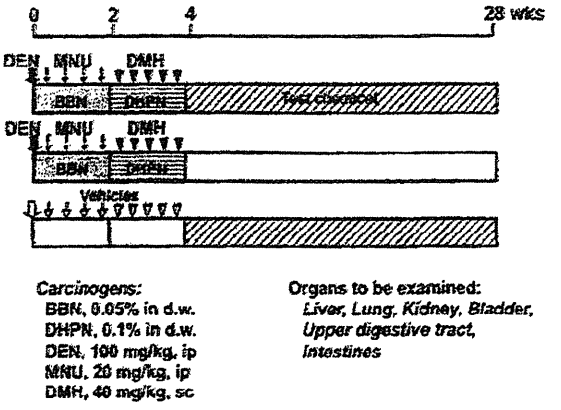

FIGURE 4.—Protocol of The Ito Multi-organ Model (DMBDD Model). Six-week-old F344 male rats are given i.p. injections of diethylnitrosamine (DEN, 100 mg/kg body wt.) and N-methylnitrosourea (MNU, 20 mg/kg body wt.), s.c. injections of 1,2-dimethylhydrazine (DMH, 40 mg/kg body wt.), and 0.05% N-butyl-N-(4-hydroxybutyl)nitrosamine (BBN) and 0.1% 2,2'-dihydroxy-di-n-propylnitrosamine (DHPN), both in the drinking water, for a total initiation period of 4 weeks (DMBDD treatment). The test compound is then administered for the following 24 weeks. The rats are sacrificed at the end of week 28. The liver, lung, thyroid, kidney, bladder, upper digestive tract (esophagus and forestomach), and intestines are examined for preneoplastic and neoplastic lesions and compared with the control rats.

2-acetylaminofluorene, 3'-methy-4-diaminoazobenzene, and ethionine (Hagiwara et al. 1993).

A total of 159 compounds were examined using the Ito Liver Model. They are classified into three categories (Table 1): (1) hepatocarcinogens; (2) carcinogens targeting organs other than the liver (nonhepatocarcinogens); and (3) compounds negative for carcinogenicity in 2-year tests in rats and mice (noncarcinogens). The compounds can also be divided into three categories according to their reported mutagenicity: mutagenic compounds, nonmutagenic compounds, and compounds with unknown mutagenic potential. Comparisons of the results obtained using the Ito Liver Model and reported *Salmonella* mutagenicity and long-term carcinogenicity testing are summarized in Table 1. It is especially noteworthy that the Ito

TABLE 2.—Results of 44 Compounds in the Medium-term Multi-organ Carcinogenesis Bioassay (DMD/DMBDD Model)

	Positive Compounds/Examined (%)			
	Mutagenicity (Ames test)			
Test compounds	Positive	Negative	Unknown	Total
Liver carcinogen	12/12(100)	5/5(100)	0/0(0)	17/17(100)
Non-liver carcinogen	10/11(91)[a]	8/10(80)[b]	1/1(100)	19/22(86)
Not carcinogenic	0/1(0)	0/4(0)	0/0(0)	0/5(0)

[a] One negative compound is Benzo[a]pyrene.
[b] Two negative compounds are Sesamol and Daminozide.

Liver Model identified 59 of 64 (92%) liver carcinogens, irrespective of their mutagenicity, leaving only 5 false negatives; 30 out of 31 (97%) mutagenic and 29 out of 33 (88%) nonmutagenic hepatocarcinogens were identified. Three out of the four nonmutagenic carcinogens that gave false negative results were carcinogenic peroxisome proliferators, known to suppress GST-P expression. It is noteworthy that the false-positive and false-negative rates are 2.1% and 3.1%, respectively. It was also noted that many chemicals positive in the Ito Liver Model were hepatotoxins (Ward et al. 1989). These results clearly demonstrate that this medium-term liver bioassay is excellent for detection of liver carcinogens (Ito, Tamano, and Shirai 2003; Shirai 1997).

A formula for the validity of carcinogen screening tests is described by Cooper, Saracci, and Cole (1979). This formula evaluates five categories: sensitivity, specificity, predictive value (positive predictivity), false-positive rate, and false-negative rate of the screening test. When the Ito Liver Model was evaluated, all five categories demonstrated excellent values (Shirai, Hirose, and Ito 1999). The Ito Liver Model was accepted as an alternative protocol to replace one of the 2-year chronic administration assays at the Fourth International Conference on Harmonization (ICH Steering Committee 1997).

Ito Multi-organ Model (DMBDD Model)

The Ito Multi-organ Model was developed for the detection of carcinogens not identified by the Ito Liver Model. F344 male rats are given i.p. injections of diethylnitrosamine (DEN, 100 mg/kg body wt.) and N-methylnitrosourea (MNU, 20 mg/kg body wt.), s.c. injections of 1,2-dimethylhydrazine (DMH, 40 mg/kg body wt.), and 0.05% N-butyl-N-(4-hydroxybutyl)nitrosamine (BBN) and 0.1% 2,2'-dihydroxy-di-n-propylnitrosamine (DHPN), both in the drinking water, for a total initiation period of 4 weeks (DMBDD treatment) (Akagi et al. 1995; Ito et al. 1996). Then rats are given the test compound in the diet or drinking water or by injection for the following 24 weeks. The animals are sacrificed at the end of week 28 (Figure 4). The organs targeted by the 5 different carcinogens—the liver, lung, thyroid, kidney, bladder, upper digestive tract (esophagus and forestomach), and intestines—are histologically examined for preneoplastic and neoplastic lesion development (Fukushima et al. 1991; Ito et al. 1996).

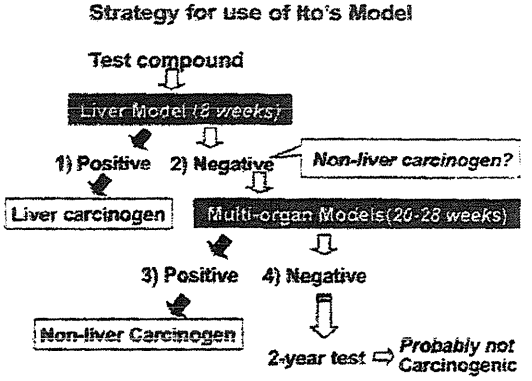

FIGURE 5.—Strategy for the Use of Ito's Model. (1) Positive compound in the liver model: is a liver carcinogen. (2) Negative compound in the liver model: test using the multi-organ model. (3) Positive compound in the multi-organ model: is a carcinogen. (4) Negative in both the liver and multi-organ models: is probably not carcinogenic.

A total of 44 compounds were examined using the Ito Multi-organ Model. A summary of the results is presented in Table 2. All 17 liver carcinogens tested positive, including peroxisome proliferators, and 19 of 22 nonliver carcinogens (86%) tested positive. The Ito Multi-organ Model was able to identify carcinogens irrespective of their mutagenicity; 22 of 23 mutagenic carcinogens and 13 of 15 nonmutagenic carcinogens were identified (Table 2).

The medium-term bioassay described here is a rapid, reliable, and practical tool for the prediction of the carcinogenic potential of chemicals. The strategy for the use of the Ito Model is presented in Figure 5.

1. Positive in liver model: carcinogen.
2. Negative in liver model: apply the multi-organ model.
3. Positive in the multi-organ model: carcinogen.
4. Negative in both the liver and multi-organ models: probably not carcinogenic.

The system is now internationally well recognized and recommended as an alternative carcinogenicity test.

ACKNOWLEDGMENTS

We would like to thank the following scientists for their contributions to the establishment of the medium-term liver bioassay: Shoji Fukushima, Masae Tatematsu, Masao Hirose, Ryohei Hasegawa, Akihiro Hagiwara, Masashi Sano, Mayumi Kawabe, Satoru Takahashi, Makoto Asamoto, Toshio Kato, Tadashi Ogiso, Koji Kato, Kumiko Ogawa, Mitsuru Futakuchi, Masato Ohshima, Keisuke Nakanishi, Witaya Thamavit, Ross Cameron, Joao L. de Camargo, Ricardo Cabral, Dae Joong Kim, Jerrold M. Ward, and Malcolm A. Moore. The authors express deep gratitude to Dr. David B. Alexander of Tsuda's department for valuable advice and language editing.

REFERENCES

Akagi, K., Hirose, M., Hoshiya, T., Mizoguchi, Y., Ito, N., and Shirai, T. (1995). Modulating effects of ellagic acid, vanillin and quercetin in a rat medium term multi-organ carcinogenesis model. *Cancer Lett* **94**, 113–21.

Ashby, J., and Tennant, R. W. (1991). Definitive relationships among chemical structure, carcinogenicity and mutagenicity for 301 chemicals tested by the U.S. NTP. *Mutat Res* **257**, 229–306.

Bannasch, P. (1986). Preneoplastic lesions as end points in carcinogenicity testing. I. Hepatic preneoplasia. *Carcinogenesis* **7**, 689–95.

Cooper, J. A., 2nd, Saracci, R., and Cole, P. (1979). Describing the validity of carcinogen screening tests. *Br J Cancer* **39**, 87–89.

Fukushima, S., Hagiwara, A., Hirose, M., Yamaguchi, S., Tiwawech, D., and Ito, N. (1991). Modifying effects of various chemicals on preneoplastic and neoplastic lesion development in a wide-spectrum organ carcinogenesis model using F344 rats. *Jpn J Cancer Res* **82**, 642–49.

Hagiwara, A., Tanaka, H., Imaida, K., Tamano, S., Fukushima, S., and Ito, N. (1993). Correlation between medium-term multi-organ carcinogenesis bioassay data and long-term observation results in rats. *Jpn J Cancer Res* **84**, 237–45.

Hasegawa, R., and Ito, N. (1992). Liver medium-term bioassay in rats for screening of carcinogens and modifying factors in hepatocarcinogenesis. *Food Chem Toxicol* **30**, 979?2.

Higginson, G., and Anderson, R. (1931). Experimental pathology of the liver. 1. Restoration of the liver of the white rat following partial surgical removal. *Arch Pathol* **12**, 186–202.

ICH Steering Committee, I. (1997). International Conference on Harmonization: Carcinogenicity: testing for carcinogenicity of pharmaceuticals. In Proceedings of Fourth International Conference on Harmonization.

Ito, N., Hasegawa, R., Imaida, K., Hirose, M., and Shirai, T. (1996). Medium-term liver and multi-organ carcinogenesis bioassays for carcinogens and chemopreventive agents. *Exp Toxicol Pathol* **48**, 113–19.

Ito, N., Hasegawa, R., Imaida, K., Hirose, M., Shirai, T., Tamano, S., and Hagiwara, A. (1997). Medium-term rat liver bioassay for rapid detection of hepatocarcinogenic substances. *J Toxicol Pathol* 1–11.

Ito, N., Hasegawa, R., Imaida, K., Masui, T., Takahashi, S., and Shirai, T. (1992). Pathological markers for non-genotoxic agent-associated carcinogenesis. *Toxicol Lett* **64**, 613–20.

Ito, N., Tamano, S., and Shirai, T. (2003). A medium-term rat liver bioassay for rapid in vivo detection of carcinogenic potential of chemicals. *Cancer Sci* **94**, 3–8.

Kitahara, A., Satoh, K., Nishimura, K., Ishikawa, T., Ruike, K., Sato, K., Tsuda, H., and Ito, N. (1984). Changes in molecular forms of rat hepatic glutathione S-transferase during chemical hepatocarcinogenesis. *Cancer Res* **44**, 2698–2703.

Liu, L. L., Gong, L. K., Qi, X. M., Cai, Y., Wang, H., Wu, X. F., Xiao, Y., and Ren, J. (2005). Altered expression of cytochrome P450 and possible correlation with preneoplastic changes in early stage of rat hepatocarcinogenesis. *Acta Pharmacol Sin* **26**, 737–44.

Matsumoto, K., and Nakamura, T. (1992). Hepatocyte growth factor: molecular structure, roles in liver regeneration, and other biological functions. *Crit Rev Oncog* **3**, 27–54.

Oesterle, D., and Deml, E. (1990). Detection of chemical carcinogens by means of the "rat liver foci bioassay." *Exp Pathol* **39**, 197–206.

Ogawa, K., Yokokawa, K., Tomoyori, T., and Onoe, T. (1982). Induction of gamma-glutamyltranspeptidase-positive altered hepatocytic lesions by combination of transplacental-initiation and postanal-selection. *Int J Cancer* **29**, 333–6.

Ogiso, T., Tatematsu, M., Tamano, S., Tsuda, H., and Ito, N. (1985). Comparative effects of carcinogens on the induction of placental glutathione S-transferase-positive liver nodules in a short-term assay and of hepatocellular carcinomas in a long-term assay. *Toxicol Pathol* **13**, 257–65.

Peraino, C., Fry, R. J., Staffeldt, E., and Christopher, J. P. (1975). Comparative enhancing effects of phenobarbital, amobarbital, diphenylhydantoin, and dichlorodiphenyltrichloroethane on 2-acetylaminofluorene-induced hepatic tumorigenesis in the rat. *Cancer Res* **35**, 2884–90.

Peraino, C., Fry, R. J., Staffeldt, E., and Christopher, J. P. (1977). Enhancing effects of phenobarbitone and butylated hydroxytoluene on 2-acetylaminofluorene-induced hepatic tumorigenesis in the rat. *Food Cosmet Toxicol* **15**, 93–96.

Peraino, C., Staffeldt, E. F., Haugen, D. A., Lombard, L. S., Stevens, F. J., and Fry, R. J. (1980). Effects of varying the dietary concentration of phenobarbital on its enhancement of 2-acetylaminofluorene-induced hepatic tumorigenesis *Cancer Res* **40**, 3268–273.

Pitot, H., and Dragan, Y. (2001). Chemical carcinogenesis. In Casertt & Doull's TOXICOLOGY: The basic science of poisons, 6th ed. (I. K. CD, ed.), pp. 241–319. McGraw-Hill, New York.

Shirai, T. (1997). A medium-term rat liver bioassay as a rapid in vivo test for carcinogenic potential: A historical review of model development and summary of results from 291 tests. *Toxicol Pathol* **25**, 453–60.

Shirai, T., Hirose, M., and Ito, N. (1999). The use of short-and medium-term tests for carcinogens and data on genetic effects in carcinogenic hazard evaluation. Consensus report. In IARC Sci Publ, pp. 1–18.

Solt, D., and Farber, E. (1976). New principle for the analysis of chemical carcinogenesis. *Nature* **263**, 701–3.

Tatematsu, M., Mera, Y., Ito, N., Satoh, K., and Sato, K. (1985). Relative merits of immunohistochemical demonstrations of placental, A, B and C forms of glutathione S-transferase and histochemical demonstration of gamma-glutamyl transferase as markers of altered foci during liver carcinogenesis in rats. *Carcinogenesis* **6**, 1621–26.

Tatematsu, M., Shirai, T., Tsuda, H., Miyata, Y., Shinohara, Y., and Ito, N. (1977). Rapid production of hyperplastic liver nodules in rats treated with carcinogenic chemicals: a new approach for an in vivo short-term screening test for hepatocarcinogens. *Gann* **68**, 499–507.

Tsuda, H., Asamoto, M., Iwahori, Y., Hori, T., Ota, T., Baba-Toriyama, H., Uehara, N., Kim, D. J., Krutovskikh, V. A., Takasuka, N., et al. (1996). Decreased connexin32 and a characteristic enzyme phenotype in clofibrate-induced preneoplastic lesions not shared with spontaneously occurring lesions in the rat liver. *Carcinogenesis* **17**, 2441–48.

Tsuda, H., Fukushima, S., Wanibuchi, H., Morimura, K., Nakae, D., Imaida, K., Tatematsu, M., Hirose, M., Wakabayashi, K., and Moore, M. A. (2003). Value of GST-P positive preneoplastic hepatic foci in dose-response studies of hepatocarcinogenesis: Evidence for practical thresholds with both genotoxic and nongenotoxic carcinogens. A review of recent work. *Toxicol Pathol* **31**, 80–86.

Tsuda, H., Hasegawa, R., Imaida, K., Masui, T., Moore, M. A., and Ito, N. (1984). Modifying potential of thirty-one chemicals on the short-term development of gamma-glutamyl transpeptidase-positive foci in diethylnitrosamine-initiated rat liver. *Gann* **75**, 876–83.

Tsuda, H., Lee, G., and Farber, E. (1980). Induction of resistant hepatocytes as a new principle for a possible short-term in vivo test for carcinogens. *Cancer Res* **40**, 1157–64.

Tsuda, H., Moore, M. A., Asamoto, M., Inoue, T., Ito, N., Satoh, K., Ichihara, A., Nakamura, T., Amelizad, Z., and Oesch, F. (1988). Effect of modifying agents on the phenotypic expression of cytochrome P-450, glutathione S-transferase molecular forms, microsomal epoxide hydrolase, glucose-6-phosphate dehydrogenase and gamma-glutamyltranspeptidase in rat liver preneoplastic lesions. *Carcinogenesis* **9**, 547–54.

Tsuda, H., Moore, M. A., Asamoto, M., Satoh, K., Tsuchida, S., Sato, K., Ichihara, A., and Ito, N. (1985). Comparison of the various forms of glutathione S-transferase with glucose-6-phosphate dehydrogenase and gamma-glutamyltranspeptidase as markers of preneoplastic and neoplastic lesions in rat kidney induced by N-ethyl-N-hydroxyethylnitrosamine. *Jpn J Cancer Res* **76**, 919–29.

Tsuda, H., Ozaki, K., Uwagawa, S., Yamaguchi, S., Hakoi, K., Aoki, T., Kato, T., Sato, K., and Ito, N. (1992). Effects of modifying agents on conformity of enzyme phenotype and proliferative potential in focal preneoplastic and neoplastic liver cell lesions in rats. *Jpn J Cancer Res* **83**, 1154–65.

Ward, J. M., Tsuda, H., Tatematsu, M., Hagiwara, A., and Ito, N. (1989). Hepatotoxicity of agents that enhance formation of focal hepatocellular proliferative lesions (putative preneoplastic foci) in a rapid rat liver bioassay. *Fundam Appl Toxicol* **12**, 163–71.

Carcinogenesis vol.31 no.5 pp.927–935, 2010
doi:10.1093/carcin/bgq029
Advance Access publication February 25, 2010

Involvement of macrophage inflammatory protein 1α (MIP1α) in promotion of rat lung and mammary carcinogenic activity of nanoscale titanium dioxide particles administered by intra-pulmonary spraying

Jiegou Xu[1], Mitsuru Futakuchi[1], Masaaki Iigo[1], Katsumi Fukamachi[1], David B.Alexander[1], Hideo Shimizu[2], Yuto Sakai[1,3], Seiko Tamano[4], Fumio Furukawa[4], Tadashi Uchino[5], Hiroshi Tokunaga[6], Tetsuji Nishimura[5], Akihiko Hirose[6], Jun Kanno[6] and Hiroyuki Tsuda[1,*]

[1]Department of Molecular Toxicology and [2]Core Laboratory, Nagoya City University Graduate School of Medical Sciences, 1-Kawasumi, Mizuho-cho, Mizuho-ku, Nagoya 467-8601, Japan, [3]Department of Drug Metabolism and Disposition, Graduate School of Pharmaceutical Sciences, 3-1, Tanabe-Dohri, Mizuho-ku, Nagoya 467-8603, Japan, [4]DIMS Institute of Medical Science, Inc., 84 Ooura, Nishiazai, Azai-cho, Ichinomiya 491-0113, Japan, [5]National Institute of Health Sciences, 1-18-1 Kamiyoga, Setagaya-ku, Tokyo 158-8501, Japan and [6]Pharmaceuticals and Medical Devices Agency, 2-3-3, Kasumigaseki, Chiyoda-ku, Tokyo 100-0013, Japan

*To whom correspondence should be addressed. Tel: +81 52 853 8091; Fax: +81 52 853 8996; Email: htsuda@med.nagoya-cu.ac.jp

Titanium dioxide (TiO_2) is evaluated by World Health Organization/International Agency for Research on Cancer as a Group 2B carcinogen. The present study was conducted to detect carcinogenic activity of nanoscale TiO_2 administered by a novel intrapulmonary spraying (IPS)-initiation–promotion protocol in the rat lung. Female human c-Ha-*ras* proto-oncogene transgenic rat (*Hras*128) transgenic rats were treated first with *N*-nitrosobis(2-hydroxypropyl)amine (DHPN) in the drinking water and then with TiO_2 (rutile type, mean diameter 20 nm, without coating) by IPS. TiO_2 treatment significantly increased the multiplicity of DHPN-induced alveolar cell hyperplasias and adenomas in the lung, and the multiplicity of mammary adenocarcinomas, confirming the effectiveness of the IPS-initiation–promotion protocol. TiO_2 aggregates were localized exclusively in alveolar macrophages and had a mean diameter of 107.4 nm. To investigate the underlying mechanism of its carcinogenic effects, TiO_2 was administered to wild-type rats by IPS five times over 9 days. TiO_2 treatment significantly increased 8-hydroxydeoxy guanosine level, superoxide dismutase activity and macrophage inflammatory protein 1α (MIP1α) expression in the lung. MIP1α, detected in the cytoplasm of TiO_2-laden alveolar macrophages *in vivo* and in the media of rat primary alveolar macrophages treated with TiO_2 *in vitro*, enhanced proliferation of human lung cancer cells. Furthermore, MIP1α, also detected in the sera and mammary adenocarcinomas of TiO_2-treated *Hras*128 rats, enhanced proliferation of rat mammary carcinoma cells. These data indicate that secreted MIP1α from TiO_2-laden alveolar macrophages can cause cell proliferation in the alveoli and mammary gland and suggest that TiO_2 tumor promotion is mediated by MIP1α acting locally in the alveoli and distantly in the mammary gland after transport via the circulation.

Introduction

Inhalation of particles and fiber is well known to be strongly associated with increased lung cancer risk in the workplace (1,2). Although the size of fiber particles was reported to be closely related to risk (3), the precise role of particles and fibers in lung cancer induction has not yet been elucidated.

Titanium dioxide (TiO_2) particles of various sizes are manufactured worldwide in large quantities and are used in a wide range of applications. TiO_2 particles have long been considered to pose little risk to respiratory health because they are chemically and thermally stable. However, TiO_2 is classified as a Group 2B carcinogen, a possible carcinogen to humans, by World Health Organization/International Agency for Research on Cancer based on the findings of lung tumor induction in female rats (3,4). This overall evaluation includes nanoscale (≤100 nm in diameter) and larger sized classes of TiO_2. At present, the mechanism underlying the development of rat lung tumors by inhalation of TiO_2 particles is unclear.

Inhalation of TiO_2 particles can occur both at the workplace, e.g. in manufacturing and packing sites, and also outside the workplace during their use (5–7). Exposure to airborne nanoparticles has been reported to be associated with a granulomatous inflammatory response in the lung (8). Inhalation studies of nanoparticles for cancer risk assessment is urgently needed, however, due to the high cost of long-term studies, available data is severely limited (9,10). The aim of this study is to understand the mechanism underlying rat lung carcinogenesis induced by inhalation of TiO_2 particles. We choose intrapulmonary spraying (IPS) because it does not require costly facilities, allows accurate dose control and approximates long-term inhalation studies (3,11).

We initially examined whether TiO_2 particles have carcinogenic activity in the rat lung using a novel IPS-initiation–promotion protocol (12,13). For these experiments, Sprague–Dawley (SD)-derived female human c-*Ha-ras* proto-oncogene transgenic rat (*Hras*128) transgenic rats, which are known to have the same carcinogen susceptibility phenotype in the lung as wild-type rats but are highly susceptible to mammary tumor induction (14–16), were treated with *N*-nitrosobis(2-hydroxypropyl)amine (DHPN) to initiate carcinogenesis and then treated with TiO_2 by IPS. We observed a promotion effect of TiO_2 particles in lung and mammary gland carcinogenesis.

To identify factors involved in this promotion effect, wild-type SD strain rats were treated with TiO_2 by IPS for 9 days. We found macrophage inflammatory protein 1α (MIP1α) was produced by TiO_2-laden alveolar macrophages in the lungs of rats treated with TiO_2. MIP1α is a member of the CC chemokine family and is primarily associated with cell adhesion and migration of multiple myeloma cells (17). It is reported to be produced by macrophages in response to a variety of inflammatory stimuli including TiO_2 (18). In the present study, MIP1α, detected in the medium of rat primary alveolar macrophages treated with TiO_2, enhanced proliferation of human lung cancer cells *in vitro*. MIP1α was also detected in the sera and mammary adenocarcinomas of TiO_2-treated *Hras*128 rats and enhanced proliferation of rat mammary carcinoma cells.

Materials and methods

Animals

Female transgenic rats carrying the Hras128 and female wild-type SD rats were obtained from CLEA Japan Co., Ltd (Tokyo, Japan) (15). The animals were housed in the animal center of Nagoya City University Medical School, maintained on a 12 h light–dark cycle and received Oriental MF basal diet (Oriental Yeast Co., Tokyo, Japan) and water ad libitum. The research was conducted according to the Guidelines for the Care and Use of Laboratory Animals of

Abbreviations: CCR1, C-C chemokine receptor type 1; DHPN, *N*-nitrosobis (2-hydroxypropyl) amine; ERK, extracellular signal-regulated kinase; GRO, *growth-regulated oncogene*; *Hras*128 rat, *human c-Ha-ras proto-oncogene* transgenic rat; IL, interleukin; IPS, intrapulmonary spraying; MEK1, MAPK/ERK kinase1; MIP1α, macrophage inflammatory protein 1α; 8-OHdG, 8-hydroxydeoxy guanosine; PBS, phosphate-buffered saline; ROS, reactive oxygen species; SD, Sprague–Dawley; SOD, superoxide dismutase; TEM, transmission electron microscopy; TiO_2, titanium dioxide.

Nagoya City University Medical School and the experimental protocol was approved by the Institutional Animal Care and Use Committee (H17-28).

Preparation of TiO_2 and IPS

TiO_2 particles (rutile type, without coating, with a mean primary size of 20 nm) were provided by Japan Cosmetic Association, Tokyo, Japan. TiO_2 particles were suspended in saline at 250 μg/ml or 500 μg/ml. The suspension was autoclaved and then sonicated for 20 min just before use. The TiO_2 suspension was intratracheally administered to animals under isoflurane anesthesia using a Microsprayer (Series 1A-1B Intratracheal Aerosolizer, Penn-Century, Philadelphia, PA) connected to a 1 ml syringe; the nozzle of the sprayer was inserted into the trachea through the larynx and a total of 0.5 ml suspension was sprayed into the lungs synchronizing with spontaneous respiratory inhalation (IPS).

IPS initiation–promotion protocol

Thirty-three female *Hras*128 rats aged 6 weeks were given 0.2% DHPN (Wako Chemicals Co., Ltd Osaka, Japan) in the drinking water for 2 weeks and 9 rats were given drinking water without DHPN. Two weeks later, the rats were divided into four groups, DHPN alone (Group 1), DHPN followed by 250 μg/ml TiO_2 (Group 2), DHPN followed by 500 μg/ml TiO_2 (Group 3) and 500 μg/ml TiO_2 without DHPN (Group 4). The TiO_2 particle preparations were administered by IPS once every 2 weeks from the end of week 4 to week 16 (a total of seven times). The total amount of TiO_2 administered to Groups 1, 2, 3 and 4 were 0, 0.875, 1.75 and 1.75 mg per rat, respectively. Three days after the last treatment, animals were killed and the organs (brain, lung, liver, spleen, kidney, mammary gland, ovaries, uterus and neck lymph nodes) were excised and divided into two pieces; one piece was immediately frozen at −80°C and used for quantitative measurement of elemental titanium, and the other piece was fixed in 4% paraformaldehyde solution in phosphate-buffered saline (PBS) buffer adjusted to pH 7.3 and processed for light microscopic examination and transmission electron microscopy (TEM); the left lungs and inguinal mammary glands were used for elemental titanium analysis and the right lungs and inguinal mammary glands were used for microscopic examination.

IPS 9 day protocol

Twenty female SD rats (wild-type counterpart of *Hras*128) aged 10 weeks were treated by IPS with 0.5 ml suspension of 500 μg/ml TiO_2 particles in saline five times over a 9 day period (Figure 2A). The total amount of TiO_2 administered was 1.25 mg per rat. Six hours after the last dose, animals were killed and the lungs and inguinal mammary glands were excised. Fatty tissue surrounding the mammary gland was removed as much as possible. The left lungs and inguinal mammary glands were used for biochemical analysis, and the right lungs were fixed in 4% paraformaldehyde solution in PBS adjusted at pH 7.3 and processed for histopathological examination and immunohistochemistry.

Light microscopic and TEM observation of TiO_2 particles in the lung

Paraffin blocks were deparaffinized and embedded in epon resin and processed for TiO_2 particle observation and titanium element analysis, using a JEM-1010 transmission electron microscope (JEOL Co. Ltd, Tokyo, Japan) equipped with an X-ray microanalyzer (EDAX, Tokyo, Japan). Size analysis of TiO_2 particles was performed using TEM photos by an image analyzer system, (IPAP, Sumika Technos Corporation, Osaka, Japan). A total of 452 particles from alveolar macrophages from rats in Group 3 (DHPN followed by 500 μg/ml TiO_2) of the IPS-initiation–promotion study and a total of 2571 particles from alveolar macrophages from rats in the IPS 9 day study were measured.

Biochemical element analysis of titanium

For the detection of elemental titanium, frozen tissue samples of 50–100 mg were digested with 5 ml concentrated HNO_3 for 22 min in a microwave oven. Titanium in the digested solutions was determined by inductively coupled plasma-mass spectrometry (HP-4500, Hewlett-Packard Co., Houston, TX) under the following conditions: RF power, 1450 W; RF refraction current, 5 W; Plasma gas current, 15 l/min; Carrier gas current, 0.91 l/min; Peri pump, 0.2 r.p.s.; Monitoring mass-m/z 48 (Ti); Integrating interval, 0.1 s; Sampling period 0.31 s.

Analysis of superoxide dismutase activity, 8-hydroxydeoxy guanosine and cytokine levels

For the analyses of superoxide dismutase (SOD) activity, 8-hydroxydeoxy guanosine (8-OHdG) and cytokine levels, animals exposed to TiO_2 particles for 9 days were used. For 8-OHdG levels, genomic DNA was isolated from the left lung and inguinal mammary gland with a DNA Extractor WB Kit (Wako Chemicals Co. Ltd). 8-OHdG levels were determined with an 8-OHdG ELISA Check Kit (Japan Institute for the Control of Aging, Shizuoka, Japan) and by a custom service (OHG Institute Co., Ltd, Fukuoka, Japan). For the analysis of SOD activity and inflammation-related cytokines, tissue from the left lung and inguinal mammary glands was excised and rinsed with cold PBS three times and homogenized in 1 ml of T-PER, Tissue Protein Extraction Reagent (Pierce, Rockford, IL), containing 1% (vol/vol) proteinase inhibitor cocktail (Sigma-Aldrich, St Louis, MO). The homogenates were clarified by centrifugation at 10 000*g* for 5 min at 4°C. Protein content was measured using a BCA™ Protein Assay Kit (Pierce). SOD activity was determined using an SOD Assay Kit (Cayman Chemical Co., Ann Arbor, MI). The levels of interleukin (IL)-1α, IL-1β, IL-6, granulocyte-macrophage colony-stimulating factor, granulocyte colony-stimulating factor, tumor necrosis factor α, interferon γ, IL-18, monocyte chemotactic protein 1 and MIP1α, growth-regulated oncogene (GRO) and vascular endothelial growth factor were measured by Multiplex Suspension array (GenoticLab Co., Ltd, Sapporo, Japan).

Immunohistochemistry

CD68 and MIP1α were detected using anti-rat CD68 (BMA Biomedicals, Augst, Switzerland) and anti-rat MIP1α polyclonal antibodies (BioVision, Lyon, France). Both antibodies were diluted 1:100 in blocking solution and applied to slides, and the slides were incubated at 4°C overnight. The slides were then incubated for 1 h with biotinylated species-specific secondary antibodies diluted 1:500 (Vector Laboratories, Burlingame, CA) and visualized using avidin-conjugated alkaline phosphatase complex (ABC kit, Vector Laboratories) and Alkaline Phosphatase Substrate Kit (Vector Laboratories).

Isolation of primary alveolar macrophages and preparation of conditioned media

Wild-type female SD rats were given 0.5 ml 6% thioglycollate medium (Thioglycollate Medium II, Eiken Chemical Co., Ltd, Tokyo, Japan) by IPS on days 1, 3 and 5, and 6 h after the last treatment, the lungs were excised and minced with sterilized scissors in RPMI 1640 containing 10% fetal bovine serum (Wako Chemicals Co., Ltd) and antibiotics. The homogenate was washed twice and plated onto 6 cm dishes and incubated for 2 h at 37°C, 5% CO_2. The dishes were then washed with PBS three times to remove unattached cells and cell debris. Samples of the remaining adherent cells were cultured in chamber slides and immunostained for CD68 to confirm their identity as macrophages; ~98% of the cells were positive for CD68.

Primary alveolar macrophages were treated with vehicle or TiO_2 particles in saline suspension at a final concentration of 100 μg/ml and then incubated for 24 h in a 37°C, 5% CO_2 incubator. The conditioned medium was collected and diluted 5-fold with RPMI 1640; the conditioned medium had a final concentration of 2% fetal bovine serum.

Western blotting

For the detection of MIP1α, aliquots of 20 μg protein from the extracts of lung or mammary tissue were separated by 15% sodium dodecyl sulfate-polyacrylamide gel electrophoresis, transferred to nitrocellulose membranes and immunoblotted. For the detection of C-C chemokine receptor type 1 (CCR1), 10% sodium dodecyl sulfate-polyacrylamide gel electrophoresis was used for the separation. Membranes were probed overnight at 4°C with anti-rat MIP1α polyclonal antibody (BioVision) diluted at 1:100 or anti-CCR1 (Santa Cruz Biotechnology, Santa Cruz, CA) diluted at 1:100. The blots were washed and incubated for 1 h with biotinylated anti-species-specific secondary antibodies (Amersham Biosciences, Piscataway, NJ) and then visualized using ECL Western Blotting Detection Reagent (Amersham Biosciences). To ensure equal protein loading, the blots were striped with Restore Western Blot Stripping Buffer (Pierce) and reprobed with anti-β actin antibody (dilution 1:2000; Sigma-Aldrich) for 1 h at room temperature.

For the detection of serum MIP1α, GRO and IL-6, aliquots of 150 μg of protein from the sera of rats treated with TiO_2 for 16 weeks were subjected to sodium dodecyl sulfate-polyacrylamide gel electrophoresis. Anti-human GRO polyclonal antibody (BioVision) and anti-mouse IL-6 polyclonal antibody (Santa Cruz) were diluted 1:100. For detection of activated extracellular signal-regulated kinase (ERK) 1/2 and total ERK1/2, phospho ERK1/2 antibody (Cell signaling Technology, Beverly, MA) and ERK1/2 antibody (Upstate, Lake placid, NY) were diluted 1:2000 and 1:25 000, respectively. The conditioned medium from alveolar macrophages, prepared as described above, was also subjected to western blot assay for MIP1α detection as described above. The blots were striped with Restore Western Blot Stripping Buffer (Pierce) and stained with Ponceau S solution (Sigma-Aldrich) for 10 min. The major band at 66 kDa was judged to be albumin and used as an internal control.

In vitro cell proliferation assay

A549 cells, a human lung cancer cell line, and the rat mammary cancer cell line C3 (19), derived from the *Hras*128 transgenic rats, were used in the *in vitro* cell proliferation assays. A549 or C3 cells were seeded into 96-well culture plates at 5×10^3 cells per well in 2% fetal bovine serum Dulbecco's modified Eagle's medium (Wako Chemicals Co., Ltd). After overnight incubation, the cells were treated as noted below, incubated for 72 h and the relative cell number was then determined.

To investigate the effect of culture supernatant from alveolar macrophages on A549 cell proliferation, their media were replaced with diluted conditioned medium, and the cells were incubated for 72 h with 0, 5, 10 and 20 μg/ml of anti-MIP1α neutralizing antibody (R&D Systems, Minneapolis, MN) or with 20 μg/ml of irrelevant IgG. To investigate the effect of recombinant cytokines on A549 cell proliferation, 10, 50 or 100 ng/ml of recombinant protein, rat MIP1α (R&D Systems), human GRO (R&D Systems) or human IL-6 (R&D Systems), was added to A549 cells. To investigate the role of ERK in MIP1α-stimulated cell proliferation, A549 cells, treated with or without 2×10^{-7} M of the specific MAPK/ERK kinase1 (MEK1) inhibitor PD98059 (Cell Signaling Technology) for 10 min, were treated with 50 ng/ml of MIP1α protein. To investigate the effect of reactive oxygen species (ROS) on cell proliferation, A549 cells, with or without pretreatment with 1 mM *N*-acetyl cysteine (Wako Chemicals Co. Ltd) for 30 min, were treated with 0.5 mM H_2O_2 (Wako Chemicals Co. Ltd). To investigate of the effects of MIP1α on rat mammary cells, C3 cells were treated with serially diluted recombinant rat MIP1α (0, 0.4, 2.0, 10 and 50 ng/ml, respectively; R&D Systems). For detecting the direct effect of TiO_2 particles on A549 and C3 cell proliferation, 5×10^3 A549 or C3 cells were cultured overnight and then treated with 10 or 50 μg/ml of TiO_2 particles.

After 72 h incubation, the relative cell number of A549 and C3 was determined using the Cell Counting Kit-8 (Dojindo Molecular Technologies, Rockville, MD) according to the manufacturer's instruction.

Statistical analysis

For *in vivo* data, statistical analysis was performed using the Kruskal–Wallis and Bonferroni–Dunn's multiple comparison tests. *In vitro* data are presented as means ± standard deviations. The statistical significance of *in vitro* findings was analyzed using a two-tailed Student's *t*-test and Bonferroni–Dunn's multiple comparison tests. A value of $P < 0.05$ was considered significant. The Spearman's rank correlation test was used to determine the association between TiO_2 dose and TiO_2 carcinogenic activity.

Results

Promoting effects of TiO_2 particles in DHPN-induced lung and mammary carcinogenesis

Prior to initiation of the IPS-initiation–promotion and IPS 9 day studies, we conducted a preliminary study to confirm whether IPS would be a good tool to deliver TiO_2 particles to the alveoli. Rats were treated by IPS with India ink. We observed that ink particles of ~50 to 500 μm in diameter were diffusely distributed throughout the alveoli space (data not shown), confirming that IPS could deliver TiO_2 particles to the alveoli.

Four groups of female Hras128 rats were treated with +/− DHPN to initiate carcinogenesis and then treated with TiO_2 by IPS for 12 weeks: Group 1, DHPN alone; Group 2, DHPN followed by 250 μg/ml TiO_2; Group 3, DHPN followed by 500 μg/ml TiO_2 and Group 4, 500 μg/ml TiO_2 without DHPN. Microscopic observation in the lung showed scattered inflammatory foci, alveolar cell hyperplasia (Figure 1A) and adenomas in the DHPN-treated rats. The multiplicity (numbers per square centimeter lung) of hyperplasias and adenomas in Group 3 (DHPN followed by 500 μg/ml TiO_2) were significantly increased compared with Group 1 (DHPN followed by saline, Table I), and the increase showed a dose-dependent correlation (rho = 0.630, $P = 0.001$ for hyperplasias and rho = 0.592, $P = 0.029$ for adenomas) by the Spearman's rank correlation test. In the mammary gland, TiO_2 treatment significantly increased the multiplicity of adenocarcinomas (Figure 1C) and tended to increase the weight of the mammary tumors (Figure 1C). In the rats, which received TiO_2 treatment without prior DHPN treatment, alveolar proliferative lesions were not observed although slight inflammatory lesions were observed.

TiO_2 was distributed primarily to the lung, but minor amounts of TiO_2 were also found in other organs (supplementary Figure 1A is available at *Carcinogenesis* Online).

Various sizes of TiO_2 aggregates were observed in alveolar macrophages (Figure 1B). The TiO_2-laden macrophages were evenly scattered throughout the lung alveoli. The number of hyperplasias with TiO_2-laden macrophages was dose dependently increased (supplementary Table 1 is available at *Carcinogenesis* Online). This result suggests that TiO_2-laden macrophages may be involved in the promotion of alveolar hyperplasia.

The size distribution of TiO_2 particle aggregate is shown in Figure 1D. Of 452 particle aggregates examined, 362 (80.1%) were nanosize, i.e. <100 nm. Overall, the average size was 84.9 nm and the median size was 44.4 nm.

IPS 9 day study—analysis of TiO_2

Female SD rats were treated with TiO_2 by IPS over a 9 day period (Figure 2A). Microscopic observation showed scattered inflammatory lesions with infiltration of numerous macrophages mixed with a few neutrophils and lymphocytes in TiO_2-treated animals. Overall, the number of macrophages in the alveoli was significantly increased in the TiO_2-treated animals (Figure 2B). As expected from the results of the IPS-initiation–promotion study, alveolar proliferative lesions were not observed (Figure 2C).

Morphologically, TiO_2 particles were observed as yellowish, polygonal bodies in the cytoplasm of cells (Figure 2D). These cells are morphologically distinct from neutrophils and strongly positive for CD68 (Figure 2E), indicating that the TiO_2 engulfing cells were macrophages. TiO_2 aggregates of various sizes were found in macrophages, and aggregates larger than a single macrophage were surrounded by multiple macrophages (supplementary Figure 1B is available at *Carcinogenesis* Online).

TEM also showed electron dense bodies in the cytoplasm of macrophages (Figure 2F and G). These bodies were found exclusively in macrophages and not found in the alveolar parenchyma, including alveolar epithelium and alveolar wall cells, or in any other cell type. The shape of the electron dense TiO_2 particles in the cytoplasm was quite similar to that observed in preparations taken from TiO_2 suspensions before administration (Figure 2H and supplementary Figure 1C and D is available at *Carcinogenesis* Online). Individual TiO_2 particles were rod-like in shape (supplementary Figure 1C is available at *Carcinogenesis* Online).

Element analysis by TEM and X-ray microanalysis indicated that these electron dense bodies were composed primarily of titanium particles (supplementary Figure 1E and F-1 and 1F-2 is available at *Carcinogenesis* Online). Titanium was not observed in the surrounding alveolar cells without electron dense bodies (supplementary Figure 1F-3 is available at *Carcinogenesis* Online). The size distribution of TiO_2 particle aggregates is shown in Figure 2I. Of 2571 particle aggregates examined, 1970 (76.6%) were <100 nm and five particles were >4000 nm in size. Overall, the average size was 107.4 nm and the median size was 48.1 nm.

IPS 9 day study—analysis of oxidative stress and inflammation-related factors in the lungs of wild-type rats

IPS of TiO_2 particles significantly increased SOD activity (Figure 3A) and 8-OHdG levels (Figure 3B) in the lungs of wild-type rats, but not in the mammary glands. Analysis of the expression levels of 12 cytokines using suspension array indicated that administration of TiO_2 particles significantly upregulated the expression of MIP1α, GRO and IL-6 in the lung tissue of wild-type rats (supplementary Table 2 is available at *Carcinogenesis* Online). MIP1α levels were slightly elevated (0.4 pg/mg protein) in the mammary gland (Figure 3C), although the elevation was not statistically significant. Elevation of MIP1α in the lung tissue of animals treated with TiO_2 particles was confirmed by western blotting (Figure 3D).

Immunohistochemically, MIP1α was detected in the cytoplasm of alveolar macrophages with phagocytosed TiO_2 particles (Figure 3E upper, stained in red) and these macrophages could be found in hyperplastic lesions of the lung (supplementary Figure 2A and B is available at *Carcinogenesis* Online). MIP1α was not detected in macrophages without TiO_2 particles (Figure 3E lower). Expression of CCR1, the major receptor of MIP1α, was observed in the lung; IPS of TiO_2 particles had little or no effect on CCR1 expression (supplementary Figure 2C is available at *Carcinogenesis* Online).

Effect of MIP1α on proliferation of a human lung cancer cell line in vitro

Alveolar macrophages were isolated from the lungs of SD rats and were confirmed to be macrophages by morphology and CD68 staining

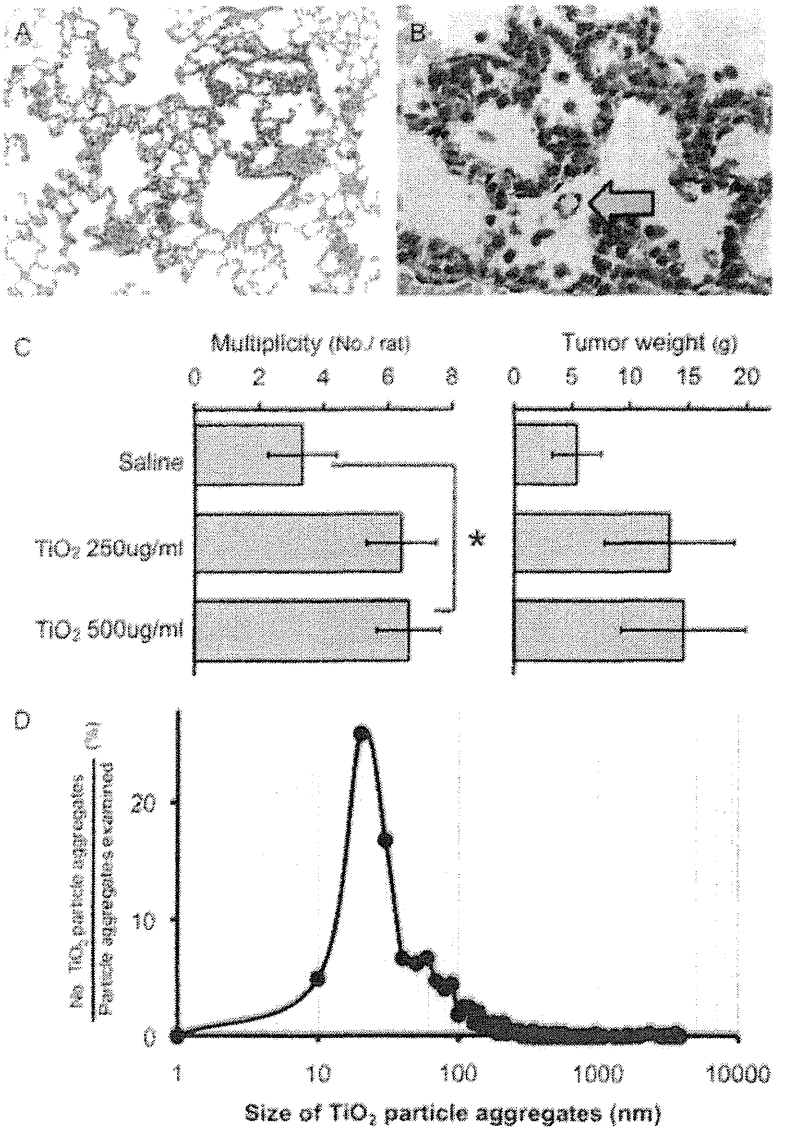

Fig. 1. Promoting effects of TiO_2 particles in DHPN-induced lung and mammary carcinogenesis (A) Alveolar hyperplasias observed in the lung of an *Hras*128 rat receiving DHPN and 500 μg/ml TiO_2 particles. (B) Alveolar macrophages with TiO_2 particles were also observed in hyperplasia lesions. (C) IPS of TiO_2 particles significantly increased the multiplicity of adenocarcinomas in the mammary gland and tended to increase the size of mammary tumors. (D) The size distribution of TiO_2 particle aggregates: among 452 particle aggregates examined, 362 (80.1%) were nanosize, i.e. ≤100 nm in diameter.

(data not shown). The macrophages were treated with TiO_2 particles suspended in saline (Figure 4A). TiO_2 induced secretion of MIP1α into the culture media (Figure 4B), and the culture medium collected from macrophages treated with TiO_2 particles promoted proliferation of A549 cells, whereas culture media collected from unexposed macrophages did not (Figure 4C). MIP1α neutralizing antibodies attenuated the promotion of A549 proliferation in a dose-dependent manner (Figure 4C). MIP1α-induced cell proliferation was also significantly suppressed by the ERK inhibitor PD98059 (Figure 4D). In addition, MIP1α increased ERK phosphorylation and PD98059 diminished ERK phosphorylation (Figure 4E).

We also examined the effect of MIP1α, GRO and IL-6, H_2O_2 and TiO_2 on the proliferation of A549 cells. MIP1α increased cell proliferation in a dose-dependent fashion, but GRO and IL-6 did not (supplementary Figure 3A–C is available at *Carcinogenesis* Online). H_2O_2 significantly suppressed cell proliferation, and antioxidant treatment diminished this suppression. Antioxidant treatment did not affect MIP1α-induced cell proliferation (supplementary Figure 3D is available at *Carcinogenesis* Online). These results suggest that ROS have no effect on tumor cell growth in this experiment.

In addition, TiO_2 did not directly increase proliferation of A549 cell (supplementary Figure 3E is available at *Carcinogenesis* Online).

Mechanism analysis of the promotion of mammary carcinogenesis

MIP1α was markedly elevated in the serum of the *Hras*128 rats treated with TiO_2 particles (Figure 5A). Serum levels of IL-6 were not changed by TiO_2 treatment and GRO was not detected in the serum

Table 1. Effect of TiO2 on incidence and multiplicity of DHPN-induced alveolar hyperplasia and adenoma of the lung

Treatment	No. of rats	Alveolar hyperplasia		Lung adenoma	
		Incidence (%)	Multiplicity ## (no./cm²)	Incidence (%)	Multiplicity # (no./cm²)
Saline	9	9 (100)	5.91 ± 1.19	0	0
$nTiO_2$ 250 mg/ml	10	10 (100)	7.36 ± 0.97*	1 (10)	0.10 ± 0.10
$nTiO_2$ 500 mg/ml	11	11 (100)	11.05 ± 0.87**	4 (36)	0.46 ± 0.21*

*$P < 0.05$, **$P < 0.001$ versus saline control.
#$P < 0.05$, ##$P < 0.001$ in trend test (Spearman's rank correlation test).

(Figure 5A). MIP1α was slightly elevated in the mammary glands of these animals (Figure 5B); possibly, the elevated MIP1α detected in the mammary tissue was due to contamination by MIP1α in the serum. Recombinant MIP1α promoted the proliferation of C3 cells in a dose-dependent manner; a slight induction could be seen at a dose of 400 pg/ml and became statistically significant at the dose of 50 ng/ml (Figure 5C). Expression of CCR1, the major receptor of MIP1α, was observed in mammary tissue, and as in the lung, IPS of TiO_2 particles had little or no effect on CCR1 expression (data not shown). TiO_2 did not directly increase proliferation of C3 cells (supplementary Figure 3F is available at *Carcinogenesis* Online).

Discussion

To elucidate the mechanism underlying rat lung carcinogenesis by TiO_2 inhalation, we chose IPS. Although this method may be less physiological than the aerosol inhalation system, we observed that agglomerates and aggregates of TiO_2 particles from nano to micro size (mean diameter 107.4 nm) were diffusely distributed throughout the lung including peripheral alveoli, and they did not cause obstruction of the terminal bronchioles. Accordingly, IPS of TiO_2 particles can be expected to act similarly to aerosol inhalation of TiO_2.

Occupational exposure limits for TiO_2 in 13 countries or regions are 5–20 mg/m³ (20), which results in TiO_2 exposure limits of 0.27–1.07 mg/kg body wt/day; calculations based on the human respiratory volume. In the present study, a total of 1.75 mg was administered per rat for 12 weeks in the high-dose group, resulting in a dose of 0.104 mg/kg body wt/day. Therefore, the dose we used in the present study was lower than the occupational exposure limit.

TiO_2, nanoscale and larger sized is evaluated as a Group 2B carcinogen by World Health Organization/International Agency for Research on Cancer (4) based on 2 year animal aerosol inhalation studies (3). We conducted the present carcinogenesis study using a two-step initiation–promotion protocol as a surrogate for a 2 year long-term protocol. Our study demonstrated that TiO_2 particles increased the multiplicity of alveolar cell hyperplasia and adenoma in the two-step IPS-initiation–promotion protocol. We used these lesions as endpoints in carcinogenicity testing because chemically induced tumors appear to be derived from hyperplasic lesions that progress to adenoma and carcinoma (21).

Several bioassay protocols based on the two-step carcinogenesis theory have been developed as practical and sensitive assays, and the compounds that exhibit promotion activity are considered to be carcinogens (22–29). Thus, our experimental design may be a practical surrogate for the long-term lung carcinogenesis protocol.

It should be noted that proliferative lesions including alveolar cell hyperplasia and adenomas were not found in the groups subjected to TiO_2 particle administration without prior treatment of DHPN. This is due to the weak carcinogenic potential and short duration of exposure to TiO_2 particles. Using the two-step IPS-initiation–promotion protocol, however, we did observe carcinogenic activity by this weak carcinogen. Thus, the two-step IPS-initiation–promotion protocol is an appropriate system to study carcinogenesis of TiO_2 particles and approximates long-term TiO_2 inhalation studies (3,11).

We next conducted a mechanism analysis of TiO_2 particle carcinogenesis focusing on the initial events induced by exposure to TiO_2 particles. Treatment with TiO_2 resulted in a modest infiltration of inflammatory cells into the alveolar space and septal wall, but the primary effect was a marked increase in the number of macrophages in the alveoli, and many of these macrophages contained phagocytosed TiO_2 particles. Alveolar macrophages play an important role in deposition and clearance of mineral fibers/particles, and macrophage activity is known to be strongly associated with inflammatory reactions and carcinogenesis caused by fibers and particles in the lung, including asbestos (30–33). ROS are known to be produced by macrophages upon particle phagocytosis (34,35). Clinical and experimental studies indicate that ROS production and resultant oxidative stress play an important role in cellular and tissue damage, inflammation and fibrosis in the lung. In our study, a significant increase in the activity of SOD and 8-OHdG formation in the lung were observed, indicating increased ROS production and DNA damage. Because macrophages are unable to detoxify TiO_2 particles, the reaction against these particles would be continuous over an extended period of time. This condition is associated with high levels of ROS production (36) and tissue toxicity (37).

Cytokine analysis of the lung tissue indicated that among the 12 cytokines examined, expression of IL-6, GRO and MIP1α were significantly higher in the TiO_2-treated group than in the vehicle group (supplementary Table 1 is available at *Carcinogenesis* Online). IL-6 is a pro-inflammatory cytokine that is involved in host defense as well as cancer development (38,39). IL-6 has been shown to be increased in lung tumor tissue (40,41) and in the sera of lung cancer patients (42). GRO, a member of the CXC chemokine family, has been shown to be involved in inflammatory responses, chemoattraction (43), carcinogenesis (44,45) and tumor progression (46). Thus, IL-6 and GRO may be involved in the promotion of lung carcinogenesis by TiO_2 (47).

Of the three cytokines induced by exposure to TiO_2 particles, however, we were particularly interested in MIP1α. This cytokine was not only induced in the lung tissue of TiO_2-treated rats, but, unlike IL-6 and GRO, it was also found in the serum of these animals. MIP1α is a member of the CC chemokine family and is primarily associated with cell adhesion and migration (17), proliferation and survival of myeloma cells (48). It is produced by macrophages in response to a variety of mineral particle-induced inflammatory stimuli (18). Our results indicate that expression of MIP1α by alveolar macrophages enhances the proliferation of A549 cells. Expression of CCR1, the major receptor of MIP1α, was observed in the lung tissue, rendering lung cells receptive to MIP1α induction of proliferation. Lung damage and inflammation induced by TiO_2 particles has also been reported to be associated with increased cell proliferation of lung epithelium cells (49), which is consistent with our results.

The MEK1–ERK-signaling pathway has been shown to be involved in CCR1 signaling (48). In the present study, the MEK1-specific inhibitor PD98059 suppressed MIP1α-induced cell proliferation and ERK phosphorylation. These results suggest that MEK1 is one of the downstream signaling molecules of MIP1α and the MEK1–ERK-signaling pathway may be partially involved in MIP1α signaling.

It should be noted that, in our IPS-initiation–promotion protocol, TiO_2 exposure also promoted DHPN-initiated mammary carcinogenesis. Our results suggest that MIP1α secreted by alveolar macrophages and transported via the circulatory system caused

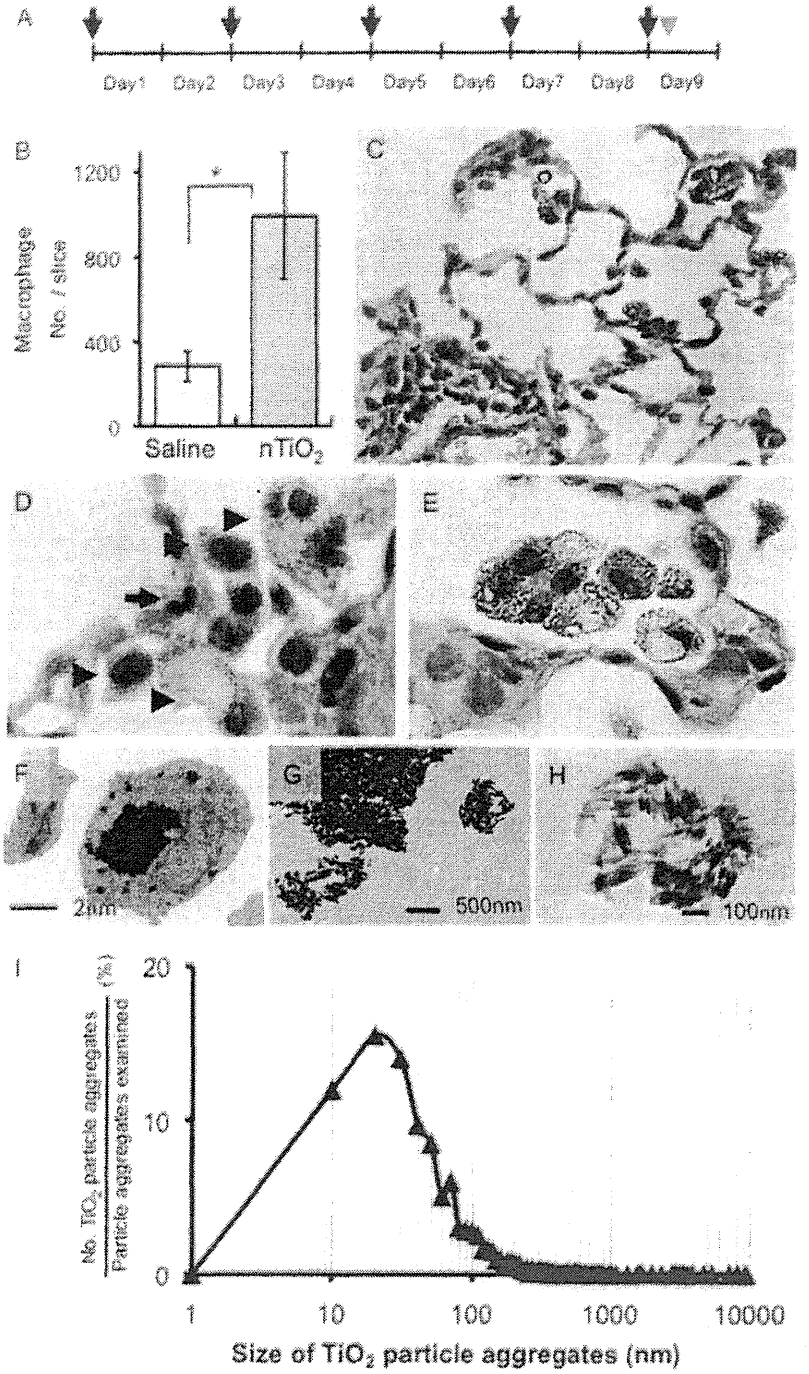

Fig. 2. TiO_2 particles in alveolar macrophages by light and electron microscopy (**A**) Twenty female SD rats (wild-type counterpart of Hras128) aged 10 weeks were treated by IPS with 0.5 ml suspension of 500 μg/ml TiO_2 particles in saline five times over a 9 day period. Arrows and arrowhead indicates IPS treatment and killing of the animals, respectively. (**B**) IPS of TiO_2 particles significantly increased the number of macrophages in the alveoli. (**C**) Inflammatory reactions were observed in the lung with slight infiltration of macrophages, neutrophils and lymphocytes. (**D**) TiO_2 particles were observed in alveolar macrophages (hematoxylin and eosin staining). Arrowheads indicate macrophages and the smaller cell indicated by the arrow is a neutrophil with its characteristic multilobular nucleus. (**E**) The multinucleated cells containing these particles were positive for the macrophage marker CD68 (Alkaline phosphatase reaction, red color). (**F**) TEM findings showed that TiO_2 particles of various sizes (~50 nm to 5 μm) were observed phagocytosed by alveolar macrophages. (**G**) Electron dense bodies were aggregates of TiO_2 particles. (**H**) TEM findings of TiO_2 particles in saline suspension before IPS. The shape of the TiO_2 particle aggregates was similar to those observed in macrophages. (**I**) The size distribution of TiO_2 particle aggregates: of 2571 particle aggregates examined, 1970 (77.1%) were <100 nm. The average size was 107.4 nm and the median size was 48.1 nm.